Decreased expression of neuropilin-1 as a novel key factor contributing to peripheral microvasculopathy and defective

(Article begins on next page)

11 July 2022

Annals of the
RHEUMATIC DISEASES
The Eular Journal

Decreased expression of neuropilin-1 as a novel key factor contributing to peripheral microvasculopathy and defective angiogenesis in systemic sclerosis

Decreased expression of neuropilin-1 as a novel key factor contributing to peripheral microvasculopathy and defective angiogenesis in systemic sclerosis

Eloisa Romano[1#*], Inês Chora[1,2#], Mirko Manetti[3#], Celestina Mazzotta[1], Irene Rosa[1,3], Silvia Bellando-Randone[1], Jelena Blagojevic[1], Raquel Soares[4], Jerôme Avouac[5], Yannick Allanore[5], Lidia Ibba-Manneschi[3], Marco Matucci-Cerinic[1], Serena Guiducci[1]

[1]Department of Experimental and Clinical Medicine, Division of Rheumatology, Azienda Ospedaliero-Universitaria Careggi (AOUC), University of Florence, Florence, Italy

[2]Department of Internal Medicine, São João Hospital Center, Al Prof Hernâni Monteiro, Porto, Portugal

[3]Department of Experimental and Clinical Medicine, Section of Anatomy and Histology, University of Florence, Florence, Italy

[4]Department of Biochemistry, Faculty of Medicine, University of Porto, Al Prof Hernâni Monteiro, Porto, Portugal

[5]Cochin Institute, Paris Descartes University, INSERM U1016 and CNRS UMR8104, Paris, France

*Correspondence to:

Eloisa Romano,
Department of Experimental and Clinical Medicine,
Division of Rheumatology,
University of Florence,
Viale Pieraccini 6,
50139 Florence, Italy
Email: eloisaromano@libero.it

[#]Eloisa Romano, Inês Chora and Mirko Manetti contributed equally to this work.

1

ABSTRACT

Objectives: In systemic sclerosis (SSc), vascular involvement is characterised by VEGF-A/VEGFR system disturbances. Neuropilin-1 (NRP1), a receptor for both class-3 semaphorins (Sema3s) and VEGF-A, is required for optimal VEGF-A/VEGFR-2 signalling. Here, we investigated the possible involvement of Sema3A/NRP1 axis in SSc.

Methods: Circulating Sema3A and soluble NRP1 (sNRP1) were measured in SSc patients and controls. NRP1 and Sema3A expression in skin biopsies was evaluated by immunofluorescence and Western blotting. NRP1 expression was assessed in SSc and healthy dermal microvascular endothelial cells (SSc-MVECs and H-MVECs), and in SSc and control endothelial progenitor cell (EPC)-derived ECs. The possible impact of transcription factor Fli1 deficiency on endothelial NRP1 expression was investigated by gene silencing. The binding of Fli1 to NRP1 gene promoter was evaluated using chromatin immunoprecipitation. Capillary morphogenesis was performed on Matrigel.

Results: Decreased sNRP1 levels in SSc were associated with active and late nailfold videocapillaroscopy patterns and digital ulcers. No difference in Sema3A was found between patients and controls. NRP1 was significantly decreased in SSc-MVECs both *ex vivo* and *in vitro*. NRP1 and Fli1 significantly decreased in H-MVECs challenged with SSc sera, while they were not different in SSc and control EPC-derived ECs. Fli1 occupied the NRP1 gene promoter and Fli1 gene silencing reduced NRP1 expression in H-MVECs. NRP1 gene silencing in H-MVECs resulted in a significantly impaired angiogenic capacity comparable to that of cells treated with SSc sera.

Conclusions: In SSc, NRP1 deficiency may be an additional factor in the perturbed VEGF-A/VEGFR-2 system contributing to peripheral microvasculopathy and defective angiogenesis.

Keywords: systemic sclerosis, neuropilin-1, Fli1, dermal microvascular endothelial cells, angiogenesis, peripheral microvasculopathy

INTRODUCTION

Systemic sclerosis (SSc, scleroderma) is a life-threatening connective tissue disorder of unknown aetiology, characterised by widespread vascular injury and dysfunction, impaired angiogenesis, immune dysregulation and progressive fibrosis of the skin and internal organs [1,2]. The dysregulation of vascular tone control, clinically evident as Raynaud's phenomenon, and microcirculatory abnormalities paralleled by nailfold capillaroscopic changes are the earliest clinical manifestations of SSc and may precede skin and visceral involvement by months or years [1-3]. The whole process is characterised by an uncontrolled regeneration of the microvasculature and subsequent loss of microvessels, due to defects in both vascular repair and expected increase in new vessel growth (angiogenesis), leading to severe peripheral ischaemic manifestations, such as digital ulcers and gangrene [2,3].

Recent studies have highlighted the anatomic and structural similarities between blood vessels and nerves [4]. The two networks are often aligned, with nerve fibers and blood vessels following parallel routes. Furthermore, both systems require precise control over their guidance and growth. Several molecules with attractive and repulsive properties have been found to modulate the guidance both of nerves and blood vessels [4]. These include the neuropilin receptors and their semaphorin ligands, as well as netrins, slits and their receptors [4]. Among these, neuropilin-1 (NRP1) was initially described as an axonally expressed receptor for secreted class-3 semaphorins (Sema3s), a family of soluble molecules which modulate the development of the nervous and vascular systems [5,6]. NRP1 also serves as specific vascular endothelial growth factor-A (VEGF-A) co-receptor on endothelial cells (ECs) and regulates VEGF receptor (VEGFR) signalling, leading to enhanced migration [7] and survival of ECs *in vitro* [8,9]. Furthermore, NRP1 has been implicated in VEGFR-2-mediated endothelial permeability [10] and in VEGF-A-induced three-dimensional EC biology, such as vessel sprouting and branching [11]. The absence of functional NRP1 in mice results in embryonic death due to impaired heart and blood vessel development, thus suggesting that this receptor plays a central regulatory role during developmental angiogenesis [4]. The exact molecular mechanisms by which NRP1 modulates VEGF-A biology remain to be elucidated. It has, however, been shown that NRP1 potentiates the VEGF-A/VEGFR-2 signalling pathways implicated in the migratory response of ECs [12].

The evidence that NRP1 functions as a receptor for both VEGF-A and Sema3s suggests that these latter may also play a role in the modulation of angiogenesis. In particular, it has been reported that Sema3A acts as an antiangiogenic molecule impairing EC adhesion, migration and survival *in vitro* [13-15], and regulates tumour-induced angiogenesis *in vivo* [16]. Moreover, Sema3A null mice

3

exhibit defects in blood vessel reshaping [15,17,18]. The molecular mechanisms underlying the antiangiogenic effects of Sema3A are complex. Hence, it was initially suggested that Sema3A competes with VEGF-A for NRP1 binding, thus inhibiting VEGF-A-induced angiogenesis. However, recent reports have also shown that Sema3A increases vascular permeability, inhibits EC proliferation, and induces apoptosis even in the absence of VEGF-A, suggesting that Sema3A may activate its own signalling pathways [19,20].

On these bases, we hypothesised that the Sema3A/NRP1 axis might play a role in the pathogenesis of SSc-related microvascular abnormalities. Therefore, the aim of the present study was to investigate whether the levels of Sema3A and NRP1 could be altered in the circulation, skin and ECs of SSc patients, as well as the mechanism explaining the dysregulated expression of these molecules and their possible contribution to the disturbed angiogenesis of SSc.

METHODS

An extended methods section is provided in the online supplementary material.

Patients, controls, serum samples and skin biopsies

Serum samples were obtained from 49 SSc patients [1] (45 women and 4 men; median age 64 years, range 37 to 80 years, and median disease duration 10 years, range 2 to 31 years) classified as limited cutaneous SSc (lcSSc; n = 32) or diffuse cutaneous SSc (dcSSc; n = 17) [21], and from 39 age-matched and sex-matched healthy individuals. All patients were clinically assessed as described elsewhere [3,22,23]. Clinicodemographic characteristics of SSc patients used for collection of serum samples are shown in online supplementary table S1. Full-thickness skin biopsies were obtained from the clinically involved skin of one-third of the distal forearm of 18 patients with SSc (15 women, 3 men; median age 48.5 years, range 29 to 73 years, and median disease duration 7.2 years, range 1 to 18 years). Skin samples from the same forearm region of 11 age-matched and sex-matched healthy donors were used as controls. Each skin biopsy was divided into two specimens and processed for immunohistochemistry and biomolecular analysis as described elsewhere [23]. The study was approved by the local institutional review board at the Azienda Ospedaliero-Universitaria Careggi (AOUC), Florence, Italy, and all subjects provided written informed consent.

4

Isolation, culture and stimulation of dermal microvascular endothelial cells (MVECs)

Dermal MVECs were isolated from biopsies of the involved forearm skin from 5 patients with dcSSc and from 5 healthy subjects, as described elsewhere [3,23]. MVECs from healthy subjects (H-MVECs) and SSc patients (SSc-MVECs) were used between the third and seventh passages in culture. For stimulation experiments, H-MVECs were grown to 70% confluence, and then were washed three times with serum-free medium and serum-starved overnight in MCDB medium supplemented with 2% FBS. Medium was removed and cells were incubated with 2% FBS-MCDB medium containing recombinant human VEGF-A165 (10 ng/ml; R&D Systems, Minneapolis, Minnesota, USA), or 10% serum from SSc patients (n = 5) and healthy subjects (n = 5) for 24 hours.

Late-outgrowth peripheral blood endothelial progenitor cell (EPC)-derived ECs

Late-outgrowth EPC-derived ECs were obtained from the peripheral blood of 15 SSc patients (13 women and 2 men; n = 9 with lcSSc and n = 6 with dcSSc; median age 60 years, range 42 to 78 years) and 8 healthy individuals (all women; median age 55 years, range 30 to 65 years), as described elsewhere [3,24,25].

Enzyme-linked immunosorbent assay (ELISA) for serum Sema3A and soluble NRP1 (sNRP1)

The levels of Sema3A and sNRP1 in serum samples were measured by commercial quantitative colorimetric sandwich ELISA (catalogue number ABIN481720 and ABIN415191, respectively; Antibodies-on line, Atlanta, Georgia, USA) according to the manufacturer's protocol. Each sample was measured in duplicate.

Immunofluorescence

Immunofluorescence on paraffin-embedded skin sections was performed as previously described [3]. For primary and secondary antibodies, refer to the online supplementary material.

Western blotting

Proteins were extracted from skin biopsies, dermal MVECs and late-outgrowth peripheral blood EPC-derived ECs as described elsewhere [3,25,26]. Western blotting was carried out according to previously published protocols [3]. For primary antibodies, refer to the online supplementary material.

5

Gene silencing of Friend leukaemia integration 1 (Fli1) and NRP1

MVECs were seeded shortly before transfection. The cells were transfected with 10 nM of Fli1 small interfering RNA (siRNA), 10 nM of NRP1 siRNA or non-silencing scrambled RNA (SCR) (Santa Cruz Biotechnology, Dallas, Texas, USA) using HiPerfect transfection reagent (Qiagen, Milan, Italy) for 72 hours.

RNA purification, cDNA synthesis and quantitative real-time PCR

Total RNA isolation from MVECs, first strand cDNA synthesis and mRNA quantification by SYBR Green real-time PCR was performed as reported elsewhere [27]. For predesigned oligonucleotide primer pairs obtained from Qiagen, refer to the online supplementary material.

Chromatin immunoprecipitation (ChIP) assay

The ChIP assay was carried out as previously described [28] using a rabbit polyclonal anti-Fli1 antibody (catalogue number ab15289, Abcam, Cambridge, UK). Putative Fli1 transcription factor binding site was predicted by Tfsitescan. The primers were as follows: NRP1 Forward, 5'-CTAGGGGTGCAGAGCGAG-3'; NRP1 Reverse, 5'-GAAGGAAGGCGCTGGGAG-3'.

In vitro capillary morphogenesis assay

In vitro capillary morphogenesis assay on Matrigel was performed according to previously published protocols [27] as detailed in the online supplementary material.

Statistical analysis

Statistical analyses were performed using the Statistical Package for Social Sciences (SPSS) software for Windows, version 20.0 (SPSS, Chicago, Illinois, USA). Data are expressed as mean $\pm$ SD or median and interquartile range (IQR). The Student's *t*-test and nonparametric Mann-Whitney *U*-test were used where appropriate for statistical evaluation of the differences between two independent groups. A p-value less than 0.05 was considered statistically significant.

RESULTS

Serum Sema3A and sNRP1 levels in SSc

No significant differences in serum levels of Sema3A were detected between SSc patients (median 2.22 ng/ml, IQR 1.84 to 3.17 ng/ml) and healthy controls (median 3.86 ng/ml, IQR 1.64 to 4.73

6

ng/ml) (figure 1A). Circulating sNRP1 levels were significantly reduced in SSc patients (median 0.22 ng/ml, IQR 0.0 to 0.6 ng/ml) compared with healthy individuals (median 0.69 ng/ml, IQR 0.0 to 2.5 ng/ml; p=0.001) (figure 1B). Next, we evaluated the possible correlation of serum sNRP1 levels with the nailfold videocapillaroscopy (NVC) pattern as a measure of peripheral microvascular involvement. sNRP1 levels were significantly decreased either in SSc patients with active (median 0.14 ng/ml, IQR 0.0 to 0.4 ng/ml) or late (median 0.09 ng/ml, IQR 0.0 to 0.72 ng/ml) NVC patterns than in controls (p=0.003 and p=0.01, respectively) (figure 1C). Conversely, no difference in serum sNRP1 was found between SSc patients with early NVC pattern (median 0.45 ng/ml, IQR 0.22 to 0.66 ng/ml) and healthy controls (figure 1C). Moreover, sNRP1 levels were significantly decreased in SSc patients with digital ulcers (median 0.06 ng/ml, IQR 0.0 to 0.27 ng/ml) compared both with patients without digital ulcers (median 0.43 ng/ml, IQR 0.17 to 0.71 ng/ml; p=0.009) and controls (p=0.001) (figure 1D). No significant association was found with other clinicodemographic and laboratory parameters or with clinical SSc subset.

Decreased expression of NRP1 in SSc dermal ECs *ex vivo* and *in vitro*

The expression of Sema3A and NRP1 protein in forearm skin biopsies from SSc patients and controls was investigated by immunofluorescence and Western blot. No significant differences in Sema3A expression were detected between SSc and control skin (figure 2A-C). On the contrary, NRP1 expression was decreased in clinically affected skin biopsies from SSc patients compared to healthy skin, in particular in dermal ECs and perivascular stromal cells (figure 3A-F). The localisation of NRP1 staining in vascular ECs was confirmed by NRP1/CD31 double immunofluorescence staining (figure 3C,F). Moreover, Western blot analysis confirmed that NRP1 protein expression levels were significantly reduced in SSc skin in respect to control skin (p<0.001) (figure 3G,H).

Western blot analysis on cultured dermal MVECs revealed that NRP1 protein expression levels were significantly reduced in SSc-MVECs compared to H-MVECs (p<0.005) (figure 4A). Moreover, NRP1 expression in H-MVECs significantly increased after treatment with healthy sera compared to basal condition, while it decreased after challenging with SSc sera (both p<0.005 *vs* basal H-MVECs). As expected, stimulation with recombinant human VEGF-A165 strongly upregulated NRP1 expression in H-MVECs (p<0.005 *vs* basal H-MVECs) (figure 4A). On the contrary, no obvious differences in NRP1 protein levels could be found between late-outgrowth EPC-derived ECs from SSc patients and healthy controls (figure 4B).

7

Fli1 deficiency contributes to the downregulation of NRP1 gene in SSc-MVECs

We next examined the potential mechanism by which NRP1 expression is downregulated in dermal SSc microvessels. As the expression of the transcription factor Fli1 is markedly downregulated at least partially *via* an epigenetic mechanism in SSc dermal ECs, and experimental endothelial Fli1 deficiency reproduces the histopathological and functional abnormalities characteristic of SSc vasculopathy [28-30], we hypothesised that endothelial Fli1 deficiency could inhibit the expression of NRP1 in SSc-MVECs.

First, we analysed Fli1 protein expression in cultured dermal MVECs and late-outgrowth EPC-derived ECs from SSc patients and controls (figure 4C,D). As shown in figure 4C, Fli1 protein expression in H-MVECs closely paralleled that of NRP1 in the different experimental conditions assayed, and was strongly downregulated in SSc-MVECs. Similarly to what observed for NRP1 expression, Fli1 protein levels did not differ between SSc and control late-outgrowth EPC-derived ECs (figure 4D).

Moreover, we examined the effect of Fli1 gene silencing on mRNA levels of the NRP1 gene in H-MVECs. As displayed in figure 4E, gene silencing of Fli1 significantly suppressed the mRNA expression levels of the NRP1 gene in H-MVECs ($p < 0.01$). In addition, ChIP analysis revealed that Fli1 occupied the promoter region of the NRP1 gene in H-MVECs (figure 4F). These results indicate that Fli1 directly targets the NRP1 gene promoter and is required for homeostatic NRP1 expression in ECs.

NRP1 deficiency contributes to the impaired angiogenesis of SSc-MVECs

To verify whether endothelial NRP1 deficiency has a role in the modulation of angiogenesis, we carried out *in vitro* capillary morphogenesis on Matrigel matrix. Consistent with previous findings [26], capillary morphogenesis was significantly impaired in SSc-MVECs compared with H-MVECs ($p < 0.01$) (figure 5). H-MVECs stimulated with healthy sera produced an abundant network of branching cords (figure 5). On the contrary, as previously reported [31,32] angiogenesis was significantly reduced upon challenge with SSc sera ($p < 0.01$ *vs* basal H-MVECs) (figure 5). The addition of recombinant human VEGF-A165 or anti-VEGF-A165b blocking antibodies to SSc sera significantly increased H-MVEC angiogenesis compared with cells treated with SSc sera alone (both $p < 0.05$) (figure 5). NRP1 gene silencing in H-MVECs resulted in a significant impairment of angiogenic capacity comparable to that of cells treated with SSc sera ($p < 0.01$ *vs* basal H-MVECs) (figure 5). Stimulation of NRP1-silenced H-MVECs with recombinant human proangiogenic

8

VEGF-A165 or antiangiogenic VEGF-A165b could only slightly increase or decrease angiogenesis, respectively (figure 5).

DISCUSSION

Here, we investigated for the first time the possible involvement of the Sema3A/NRP1 axis in the pathogenesis of SSc. Our present findings clearly demonstrate that serum levels and dermal expression of NRP1 are significantly decreased in SSc patients and that lower circulating sNRP1 levels correlate with the severity of NVC abnormalities and the presence of digital ulcers. In contrast to constitutive endothelial expression of NRP1 in healthy skin, NRP1 was found to be strongly reduced *ex vivo* in SSc dermal microvessels, and NRP1 downregulation was maintained *in vitro* in MVECs obtained from SSc dermis. On the contrary, we could not find any difference in NRP1 protein levels between peripheral blood EPC-derived ECs from SSc patients and healthy controls. This evidence suggests that the dysregulated expression of this receptor is restricted to locally injured microvasculature in an overt disease without affecting bone marrow-derived circulating endothelial progenitors. As far as Sema3A is concerned, no difference in its expression was observed between SSc and controls either in the circulation or in the cutaneous tissue.

The importance of NRP1 for vascular development is well established and shown by the generation of knockout mice, which display an embryonic lethal phenotype characterised by severe vascular defects due to impaired angiogenic sprouting and branching very much resembling the disturbed vessel morphology seen in SSc patients [4,33,34]. Moreover, conditional NRP1 knockout in ECs is associated with important cardiac and vascular defects, thus suggesting a crucial role for NRP1 in EC functions [35]. Even though NRP1 was originally identified as an adhesion molecule in the nervous system, it is more commonly studied as receptor for the neuronal guidance molecule Sema3A and as co-receptor for the VEGF-A165/VEGFR-2 complex with key roles in neuronal and vascular development [12,36]. Of note, several studies have implicated a dysfunctional VEGF-A/VEGFR-2 system in the impaired angiogenic process characteristic of SSc [2,26,37-39]. Moreover, besides VEGF-A, it is well known that a dysregulated expression of a large array of proangiogenic and antiangiogenic (angiostatic) factors present in the circulation of SSc patients may be mostly responsible for such angiogenic deficit [2,37-40].

In our study, not only we observed that the proangiogenic NRP1 receptor was constitutively downregulated in dermal SSc-MVECs, but also that treatment with SSc sera could significantly reduce NRP1 expression in H-MVECs, which is in line with the reported antiangiogenic properties

9

of SSc sera [2,31,32,37,41]. Strikingly, we also found that NRP1 gene silencing in H-MVECs resulted in a significantly impaired angiogenic process comparable to that of cells treated with SSc sera, further supporting the implication of NRP1 deficiency in the disturbed angiogenesis of SSc. Consistent with previous studies, stimulation with recombinant proangiogenic VEGF-A165 strongly upregulated NRP1 expression in H-MVECs suggesting that this growth factor cannot only activate ECs directly, but can also contribute to angiogenesis by a mechanism that involves upregulation of its homologous receptor NRP1 [36]. The findings of NRP1 downregulation in H-MVECs upon challenge with SSc sera are in agreement with the evidence that the majority of VEGF-A detected in SSc circulation is not the proangiogenic VEGF-A165, but rather the antiangiogenic VEGF-A165b isoform [26,42]. Further, it has been reported that VEGF-A165b is unable to bind the co-receptor NRP1 because the basic carboxyterminal amino acids essential for NRP1 binding are absent in this splice variant [43,44]. Interestingly, we observed that stimulation of H-MVECs silenced for the NRP1 co-receptor with proangiogenic VEGF-A165 slightly increased angiogenesis, while stimulation with VEGF-A165b isoform resulted only in a slight decrease in their angiogenic capacity. These data are consistent with the antiangiogenic action of VEGF-A165b being mainly dependent on its inability to recruit VEGFR-2/NRP1 co-receptor complex and activate downstream signalling. In a recent study, it was demonstrated that VEGF-A165 and VEGF-A165b may control the balance between VEGFR-2 recycling, degradation and signalling. In particular, due to the lack of NRP1 co-receptor binding, VEGF-A165b may induce differential intracellular vesicular trafficking of VEGFR-2 toward the degradative pathway [45]. Thus, both a switch from the proangiogenic to the antiangiogenic VEGF-A isoform and the concomitant NRP1 co-receptor downregulation may have a crucial role in the insufficient angiogenic response found in SSc (figure 6). Indeed, here we also demonstrated that both the addition of recombinant human VEGF-A165 or anti-VEGF-A165b blocking antibodies could significantly dampen the antiangiogenic effects of SSc sera on H-MVECs.

The clinical correlation of serum sNRP1 levels with the severity of SSc-related peripheral microvasculopathy also deserves discussion. Indeed, circulating levels of sNRP1 progressively decreased reaching the lowest values in SSc patients with the active and late NVC patterns, which are characterised by severe architectural changes of microvessels and progressive capillary loss with formation of avascular areas [46]. In addition, patients with active/late NVC patterns and digital ulcers showed serum sNRP1 levels significantly lower than healthy controls, whereas sNRP1 levels did not differ significantly between controls and SSc patients with early NVC pattern and lack of digital ulcers. However, since sNRP1 may be largely released by ECs, we should also consider that

10

the reduction in circulating levels of sNRP1 might be either a cause or a consequence of the disease, which is characterised by progressive loss of the peripheral microcirculation [2,3,46]. Circulating levels of sNRP1 could even serve as a biomarker reflecting the severity and progression of SSc microvasculopathy. Accordingly, further prospective studies on larger cohorts of SSc patients are warranted.

Finally, our mechanistic findings indicate that in SSc, endothelial NRP1 expression is suppressed at least partially due to Fli1 transcription factor deficiency. In fact, here we provide the first evidence that NRP1 is a member of the angiogenesis-related gene program regulated by Fli1 in dermal MVECs. In this context, the impact of Fli1 deficiency in the loss of EC integrity and the development of peripheral microvasculopathy during SSc has been well established [28-30]. Of note, it has been demonstrated that in SSc Fli1 expression is markedly suppressed at least partially through an epigenetic mechanism [29,30]. Thus, such an epigenetic modification might partly explain the persistence of the multiple downstream effects of Fli1 deficiency in an *in vitro* culture system, as supported by the downregulation of endothelial NRP1 observed *ex vivo* in SSc dermal microvessels and maintained in cultured dermal SSc-MVECs. Interestingly, NRP1 was found to be also a target of the antiangiogenic microRNA miR-320, and a dysregulated microRNA profile is being increasingly reported in SSc [47,48].

In conclusion, we shed light on NRP1 deficiency as a novel key factor contributing to peripheral microvasculopathy and defective angiogenesis in SSc. Further studies are warranted to decipher whether therapeutic modulation of VEGF-A/VEGFR-2/NRP1 co-receptor signalling might pave the way to boost angiogenesis and block the progression of peripheral microvasculopathy in SSc.

11

Competing interests

None declared.

REFERENCES

1) van den Hoogen F, Khanna D, Fransen J, *et al*. 2013 classification criteria for systemic sclerosis: an American College of Rheumatology/European League against Rheumatism collaborative initiative. *Ann Rheum Dis* 2013;72:1747-55.

2) Manetti M, Guiducci S, Ibba-Manneschi L, *et al*. Mechanisms in the loss of capillaries in systemic sclerosis: angiogenesis versus vasculogenesis. *J Cell Mol Med* 2010;14:1241-54.

3) Manetti M, Guiducci S, Romano E, *et al*. Decreased expression of the endothelial cell-derived factor EGFL7 in systemic sclerosis: potential contribution to impaired angiogenesis and vasculogenesis. *Arthritis Res Ther* 2013;15:R165.

4) Larrivée B, Freitas C, Suchting S, *et al*. Guidance of vascular development: lessons from the nervous system. *Circ Res* 2009;104:428-41.

5) He Z, Tessier-Lavigne M. Neuropilin is a receptor for the axonal chemorepellent Semaphorin III. *Cell* 1997;90:739-51.

6) Kolodkin AL, Levengood DV, Rowe EG, *et al*. Neuropilin is a semaphorin III receptor. *Cell* 1997;90:753-62.

7) Vander Kool CW, Jusino MA, Perman B, *et al*. Structural basis for ligand and heparin binding to neuropilin B domains. *Proc Natl Acad Sci USA* 2007;104:6152-7.

8) Favier B, Alam A, Barron P, *et al*. Neuropilin-2 interacts with VEGFR-2 and VEGFR-3 and promotes human endothelial cell survival and migration. *Blood* 2006;108:1243-50.

9) Wang L, Zeng H, Wang P, *et al*. Neuropilin-1-mediated vascular permeability factor/vascular endothelial growth factor-dependent endothelial cell migration. *J Biol Chem* 2003;278:48848-60.

10) Becker PM, Waltenberger J, Yachechko R, *et al*. Neuropilin-1 regulates vascular endothelial growth factor-mediated endothelial permeability. *Circ Res* 2005;96:1257-65.

11) Kawamura H, Li X, Goishi K, *et al*. Neuropilin-1 in regulation of VEGF-induced activation of p38MAPK and endothelial cell organization. *Blood* 2008;112:3638-49.

12) Koch S. Neuropilin signaling in angiogenesis. *Biochem Soc Trans* 2012;40:20-5.

13) Miao HQ, Soker S, Feiner L, *et al*. Neuropilin-1 mediates collapsin-1/semaphorin III inhibition of endothelial cell motility: functional competition of collapsin-1 and vascular endothelial growth factor-165. *J Cell Biol* 1999;146:233-42.

12

14) Guttmann-Raviv N, Shraga-Heled N, Varshavsky A, *et al.* Semaphorin-3A and semaphorin-3F work together to repel endothelial cells and to inhibit their survival by induction of apoptosis. *J Biol Chem* 2007;282:26294-305.

15) Serini G, Valdembri D, Zanivan S, *et al.* Class 3 semaphorins control vascular morphogenesis by inhibiting integrin function. *Nature* 2003;424:391-7.

16) Maione F, Molla F, Meda C, *et al.* Semaphorin 3A is an endogenous angiogenesis inhibitor that blocks tumor growth and normalizes tumor vasculature in transgenic mouse models. *J Clin Invest* 2009;119:3356-72.

17) Gu C, Rodriguez ER, Reimert DV, *et al.* Neuropilin-1 conveys semaphorin and VEGF signaling during neural and cardiovascular development. *Dev Cell* 2003;5:45-57.

18) Arese M, Serini G, Bussolino F. Nervous vascular parallels: axon guidance and beyond. *Int J Dev Biol* 2011;55:439-45.

19) Appleton BA, Wu P, Maloney J, *et al.* Structural studies of neuropilin/antibody complexes provide insights into semaphoring and VEGF binding. *EMBO J* 2007;26:4902-12.

20) Sakurai A, Doçi CL, Gutkind JS. Semaphorin signaling in angiogenesis, lymphangiogenesis and cancer. *Cell Res* 2012;22:23-32.

21) LeRoy EC, Black C, Fleischmajer R, *et al.* Scleroderma (systemic sclerosis): classification, subsets, and pathogenesis. *J Rheumatol* 1988;15:202-5.

22) Manetti M, Guiducci S, Romano E, *et al.* Increased serum levels and tissue expression of matrix metalloproteinase-12 in patients with systemic sclerosis: correlation with severity of skin and pulmonary fibrosis and vascular damage. *Ann Rheum Dis* 2012;71:1064-72.

23) Manetti M, Guiducci S, Romano E, *et al.* Differential expression of junctional adhesion molecules in different stages of systemic sclerosis. Arthritis Rheum 2013;65:247-57.

24) Avouac J, Wipff J, Goldman O, *et al.* Angiogenesis in systemic sclerosis: impaired expression of vascular endothelial growth factor receptor 1 in endothelial progenitor-derived cells under hypoxic conditions. *Arthritis Rheum* 2008;58:3550-61.

25) Avouac J, Cagnard N, Distler JH, *et al.* Insights into the pathogenesis of systemic sclerosis based on the gene expression profile of progenitor-derived endothelial cells. *Arthritis Rheum* 2011;63:3552-62.

26) Manetti M, Guiducci S, Romano E, *et al.* Overexpression of VEGF165b, an inhibitory splice variant of vascular endothelial growth factor, leads to insufficient angiogenesis in patients with systemic sclerosis. *Circ Res* 2011;109:e14-26.

27) Guiducci S, Manetti M, Romano E, *et al.* Bone marrow-derived mesenchymal stem cells from early diffuse systemic sclerosis exhibit a paracrine machinery and stimulate angiogenesis in vitro. *Ann Rheum Dis* 2011;70:2011-21.

28) Saigusa R, Asano Y, Taniguchi T, *et al.* A possible contribution of endothelial CCN1 downregulation due to Fli1 deficiency to the development of digital ulcers in systemic sclerosis. *Exp Dermatol* 2015;24:127-32.

29) Manetti M, Fli1 deficiency and beyond: a unique pathway linking peripheral vasculopathy and dermal fibrosis in systemic sclerosis. *Exp Dermatol* 2015;24:256-57.

30) Asano Y, Bujor AM, Trojanowska M, The impact of Fli1 deficiency on the pathogenesis of systemic sclerosis. *J Dermatol Sci* 2010;59:153-62.

13

31) Romano E, Bellando-Randone S, Manetti M, *et al.* Bosentan blocks the antiangiogenic effects of sera from systemic sclerosis patients: an in vitro study. *Clin Exp Rheumatol* 2015 Jun 19. [Epub ahead of print]

32) Borghini A, Manetti M, Nacci F, *et al.* Systemic sclerosis sera impair angiogenic performance of dermal microvascular endothelial cells: therapeutic implications of cyclophosphamide. *PLoS One* 2015;10:e0130166.

33) Kitsukawa T, Shimizu M, Sanbo M, *et al.* Neuropilin-semaphorin III/D-mediated chemorepulsive signals play a crucial role in peripheral nerve projection in mice. *Neuron* 1997;19:995-1005.

34) Kawasaki T, Kitsukawa T, Bekku Y, *et al.* A requirement for neuropilin-1 in embryonic vessel formation. *Development* 1999;126:4895-902.

35) Mukouyama YS, Gerber HP, Ferrara N, *et al.* Peripheral nerve-derived VEGF promotes arterial differentiation via neuropilin 1-mediated positive feedback. *Development* 2005;32:941-52.

36) Oh H, Takagi H, Otani A, *et al.* Selective induction of neuropilin-1 by vascular endothelial growth factor (VEGF): a mechanism contributing to VEGF-induced angiogenesis. *Proc Natl Acad Sci USA* 2002;99:383-8.

37) Matucci-Cerinic M, Kahaleh B, Wigley FM. Review: evidence that systemic sclerosis is a vascular disease. *Arthritis Rheum* 2013;65:1953-62.

38) Manetti M, Guiducci S, Ibba-Manneschi L, *et al.* Impaired angiogenesis in systemic sclerosis: the emerging role of the antiangiogenic VEGF(165)b splice variant. *Trends Cardiovasc Med* 2011;21:204-10.

39) Distler O, Distler JH, Scheid A, *et al.* Uncontrolled expression of vascular endothelial growth factor and its receptors leads to insufficient skin angiogenesis in patients with systemic sclerosis. *Circ Res* 2004;95:109-16.

40) Rabquer BJ, Koch AE. Angiogenesis and vasculopathy in systemic sclerosis: evolving concepts. *Curr Rheumatol Rep* 2012;14:56-63.

41) Mulligan-Kehoe MJ, Drinane MC, Mollmark J, *et al.* Antiangiogenic plasma activity in patients with systemic sclerosis. *Arthritis Rheum* 2007;56:3448-58.

42) Manetti M, Guiducci S, Romano E, *et al.* Increased plasma levels of the VEGF165b splice variant are associated with the severity of nailfold capillary loss in systemic sclerosis. *Ann Rheum Dis* 2013;72:1425-7.

43) Cébe Suarez S, Pieren M, Cariolato L, *et al.* A VEGF-A splice variant defective for heparin sulfate and neuropilin-1 binding shows attenuated signaling through VEGFR-2. *Cell Mol Life Sci* 2006;63:2067-77.

44) Kawamura H, Li X, Harper SJ, *et al.* Vascular endothelial growth factor (VEGF)-A165b is a weak in vitro agonist for VEGF receptor-2 due to lack of coreceptor binding and deficient regulation of kinase activity. *Cancer Res* 2008;68:4683-92.

45) Ballmer-Hofer K, Andersson AE, Ratcliffe LE, *et al.* Neuropilin-1 promotes VEGFR-2 trafficking through Rab11 vesicles thereby specifying signal output. *Blood* 2011;118:816-26.

46) Chora I, Guiducci S, Manetti M, *et al.* Vascular biomarkers and correlation with peripheral vasculopathy in systemic sclerosis. *Autoimmun Rev* 2015;14:314-22.

14

47) Wu YY, Chen YL, Jao YC, *et al.* miR-320 regulates tumor angiogenesis driven by vascular endothelial cells in oral cancer by silencing neuropilin 1. *Angiogenesis* 2014;17:247-60.

48) Broen JC, Radstake TR, Rossato M. The role of genetics and epigenetics in the pathogenesis of systemic sclerosis. *Nat Rev Rheumatol* 2014;10:671-81.

FIGURE LEGENDS

Figure 1. Serum levels of semaphorin3A (Sema3A) and soluble neuropilin-1 (sNRP1) determined by colorimetric sandwich ELISA. (A) Serum Sema3A levels in healthy controls and patients with systemic sclerosis (SSc). (B) Serum sNRP1 levels in healthy controls and SSc patients. (C) Serum sNRP1 levels in healthy controls and patients with SSc according to nailfold videocapillaroscopy (NVC) pattern (early, active and late). (D) Serum sNRP1 levels in healthy controls and patients with SSc according to the presence/absence of digital ulcers (DU). Data are shown as box plots. Each box represents the 25th to 75th percentiles. Lines inside the boxes represent the median. Lines outside the boxes represent the 10th and the 90th percentiles. Circles indicate outliers, and asterisks indicate the extreme values. Mann-Whitney *U*-test was used for statistical analysis.

Figure 2. Expression of semaphorin3A (Sema3A) in skin biopsies. (A and B) Representative microphotographs of skin sections from (A) healthy controls (n = 11) and (B) systemic sclerosis (SSc) patients (n = 18) immunostained for Sema3A (red) and counterstained with 4′,6-diamidino-2-phenylindole (DAPI; blue) for nuclei. Arrows indicate microvessels. Original magnification: x40. Scale bar = 50 μm. (C) Western blotting of total protein extracts from the skin of healthy subjects (n = 10) and SSc patients (n = 15). A protein band with the expected molecular weight of 90 kDa was detected with the anti-Sema3A antibody. Representative immunoblots are shown. The densitometric analysis of the bands normalised to α-tubulin is reported in the histograms. Data are mean ± SD of optical density in arbitrary units (a.u.).

Figure 3. Expression of neuropilin-1 (NRP1) in skin biopsies. (A, B, D, and E) Representative microphotographs of skin sections from (A and B) healthy controls (n = 11) and (D and E) systemic sclerosis (SSc) patients (n = 18) immunostained for NRP1 (red) and counterstained with 4′,6-diamidino-2-phenylindole (DAPI; blue) for nuclei. Arrows indicate microvessels. (C and F) Representative microphotographs of skin sections from healthy controls (C) and SSc patients (F) double immunostained for NRP1 (red) and the pan-endothelial cell marker CD31 (green) and counterstained with DAPI (blue). Original magnification: x20 (A and D), x40 (B and E), x100 (C and F). Scale bar = 100 μm (A and D), 50 μm (B and E), 10 μm (C and F). (G and H) Western blotting of total protein extracts from the skin of healthy subjects (n = 10) and SSc patients (n = 15). A protein band with the expected molecular weight of 103 kDa was detected with the anti-NRP1 antibody. Representative immunoblots are shown. The densitometric analysis of the bands normalised to α-tubulin is reported in the histograms. Data are mean ± SD of optical density in arbitrary units (a.u.).

Figure 4. (A-D) Expression of neuropilin-1 (NRP1) and Friend leukaemia integration 1 (Fli1) in dermal microvascular endothelial cells (MVECs) and late-outgrowth peripheral blood endothelial progenitor cell (EPC)-derived endothelial cells. (A and C) Western blotting of total protein extracts

15

from healthy MVECs (H-MVECs) at basal condition and treated with recombinant human vascular endothelial growth factor-A165 (VEGF-A165), or 10% serum from SSc patients (n = 5) and healthy subjects (n = 5) for 24 hours, and from basal systemic sclerosis MVECs (SSc-MVECs) assayed with anti-NRP1 (A) and anti-Fli1 (C) antibodies. Representative immunoblots are shown. The densitometric analysis of the bands normalised to α-tubulin is reported in the histograms. Data are mean ± SD of optical density in arbitrary units (a.u.). Student's *t*-test was used for statistical analysis. *p<0.005 *vs.* basal H-MVECs. Results are representative of three independent experiments performed with each one of the 5 H-MVEC and 5 SSc-MVEC lines. (B and D) Western blotting of protein lysates from control (n = 8) and SSc (n = 15) late-outgrowth EPC-derived endothelial cells assayed with anti-NRP1 (B) and anti-Fli1 (D) antibodies. Representative immunoblots are shown. The densitometric analysis of the bands normalised to α-tubulin is reported in the histograms. Data are mean ± SD of optical density in arbitrary units (a.u.). (E) mRNA levels of the Fli1 and NRP1 genes in H-MVECs transfected with Fli1 siRNA or non-silencing scrambled RNA (SCR) were measured by quantitative real-time PCR and normalised to mRNA levels of the 18S ribosomal RNA gene. The relative values compared with SCR are expressed as mean ± SD of three independent experiments. Statistical analysis was carried out with Student's *t*-test. *p<0.01 *vs.* SCR. (F) Chromatin was isolated from H-MVECs and immunoprecipitation was conducted with rabbit anti-Fli1 antibody or rabbit IgG. To exclude exogenous DNA contamination, negative controls were obtained by omitting the cell preparation in some specimens. PCR amplification was carried out using NRP1 promoter-specific primers. One representative of three independent experiments is shown.

Figure 5. *In vitro* angiogenesis. (A) Representative images of capillary morphogenesis on Matrigel after 24 hours. (B) Capillary morphogenesis of healthy and systemic sclerosis (SSc) dermal microvascular endothelial cells (H-MVECs and SSc-MVECs, respectively) quantified as percent field occupancy of capillary projections. Capillary morphogenesis of H-MVECs was evaluated at basal condition and after stimulation with sera from healthy subjects (n = 5) and SSc patients (n = 5), these latter alone or in combination with recombinant human vascular endothelial growth factor-A165 (VEGF-A165) or anti-VEGF-A165b blocking antibodies. Stimulation with VEGF-A165 added to basal medium was used as positive control of angiogenesis. H-MVECs transfected with NRP1 siRNA, at basal condition or challenged with recombinant human VEGF-A165 or VEGF-A165b, or non-silencing scrambled RNA (SCR), were also assayed. Capillary morphogenesis of H-MVECs at basal condition was set to 100%; the other results are normalised to this value. Data are the mean ± SD of three independent experiments performed in triplicate with each one of the 5 H-MVEC and 5 SSc-MVEC lines. Six to 9 photographic fields from 3 plates were scanned for each experimental point. Student's *t*-test was used for statistical analysis. *p<0.01 *vs.* basal H-MVECs; #p<0.05 *vs.* H-MVECs challenged with SSc sera. (C) mRNA levels of the NRP1 gene in H-MVECs transfected with NRP1 siRNA or non-silencing SCR were measured by quantitative real-time PCR and normalised to mRNA levels of the 18S ribosomal RNA gene. The relative values compared with SCR are expressed as mean ± SD of three independent experiments. Statistical analysis was carried out with Student's *t*-test. *p<0.01 *vs.* SCR.

Figure 6. Schematic illustration of the potential mechanisms steering dysregulated angiogenesis in systemic sclerosis (SSc). SSc is characterised by progressive loss of peripheral microvasculature and lack of compensatory angiogenesis. In most angiogenic states, vascular endothelial growth factor-A165 (VEGF-A165) interacts with VEGF receptor-2 (VEGFR-2) *via* the VEGF homology domain (VHD) and with the b1 and b2 domains of neuropilin-1 (NRP1) *via* exons 7 and 8. Co-expression of NRP1 and VEGFR-2 enhances VEGF-A165 binding to VEGFR-2, VEGFR-2 phosphorylation and downstream signalling cascades. In nonangiogenic conditions, such as SSc,

16

both a switch from proangiogenic VEGF-A165 to antiangiogenic VEGF-A165b isoform, which is unable to bind the co-receptor NRP1, and concomitant NRP1 downregulation may result in an insufficient tyrosine phosphorylation/activation of VEGFR-2 and incomplete or transient downstream signalling along with a differential intracellular vesicular trafficking of VEGFR-2 towards the degradative pathway, ultimately leading to an impaired angiogenic response.
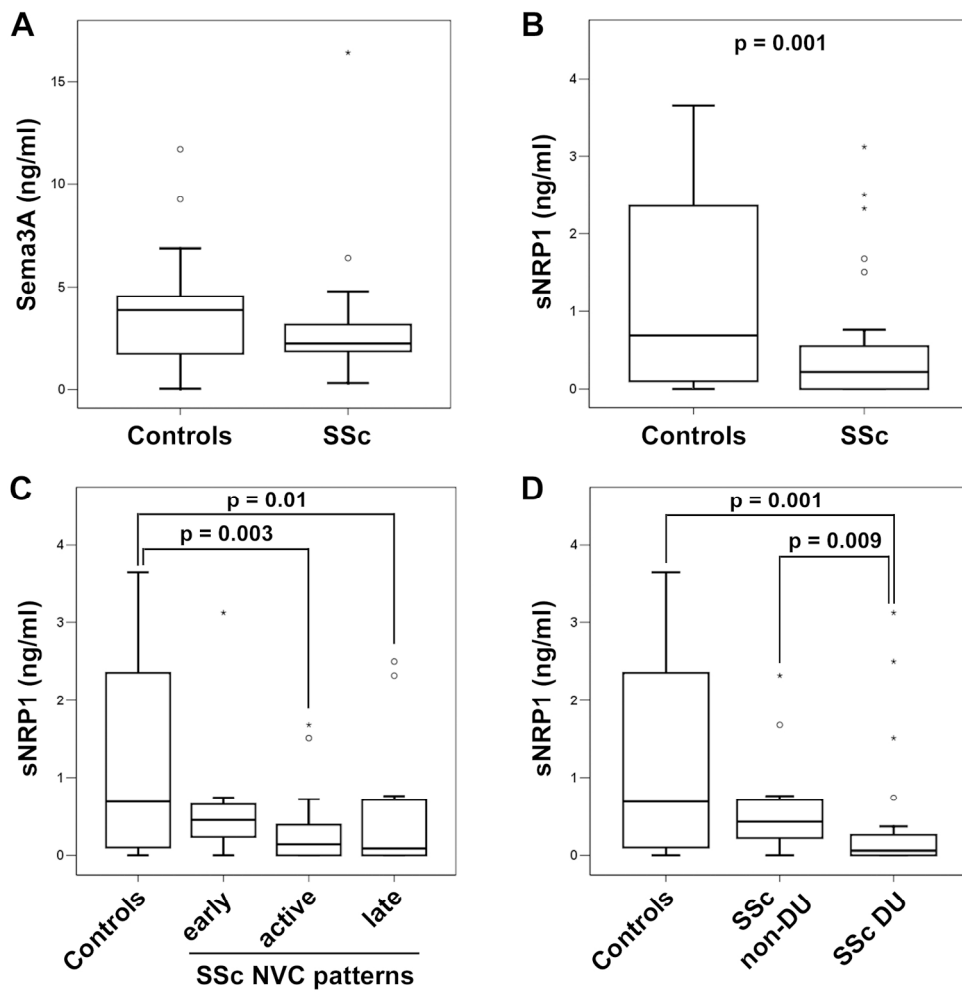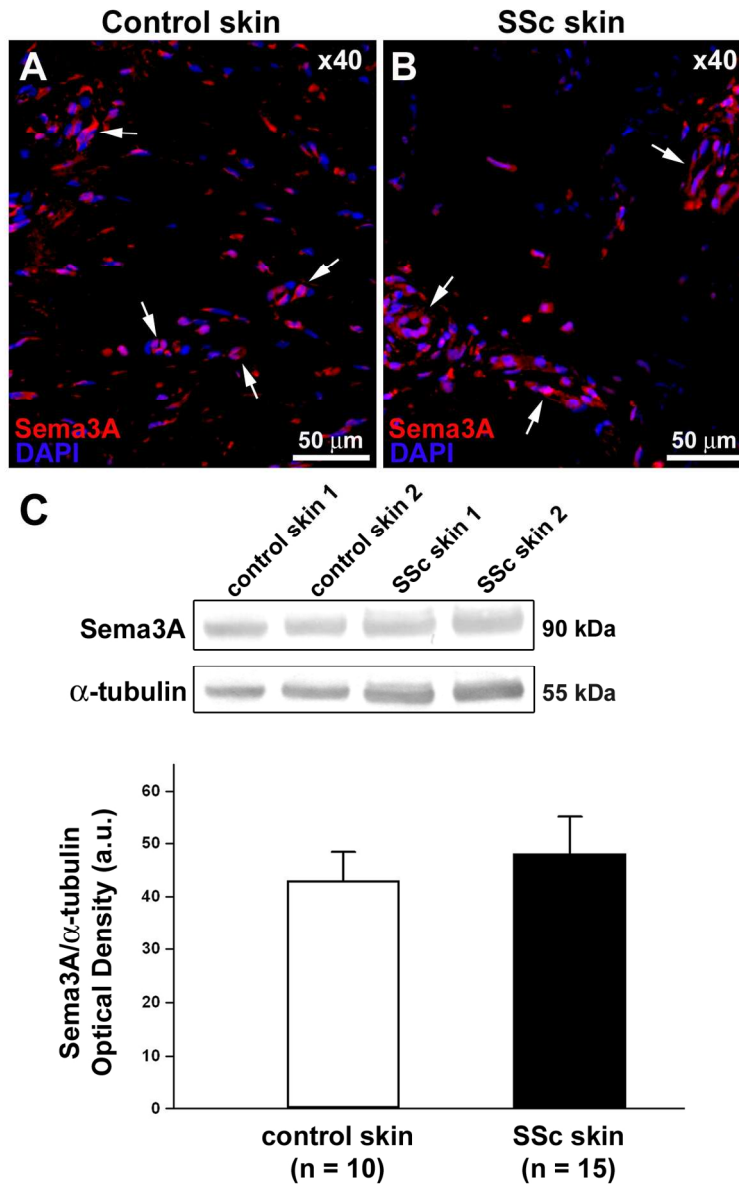
17

Figure 1
170x170mm (300 x 300 DPI)

Figure 2
115x180mm (300 x 300 DPI)
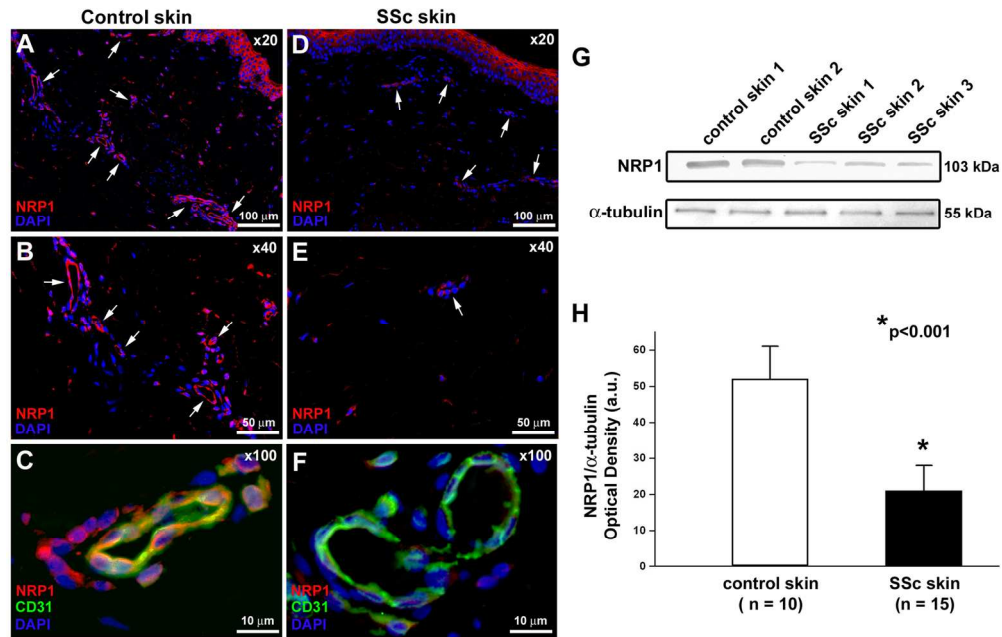
Figure 3
170x108mm (300 x 300 DPI)
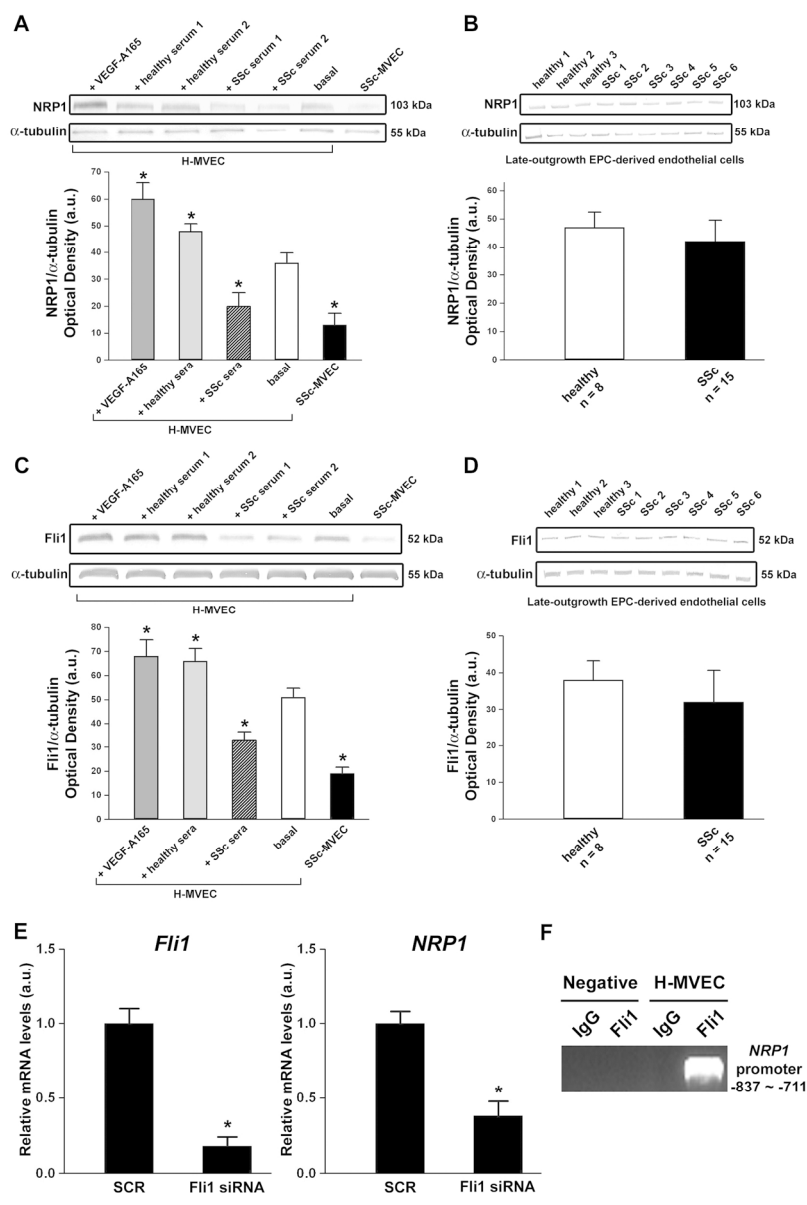
Figure 4
142x209mm (300 x 300 DPI)
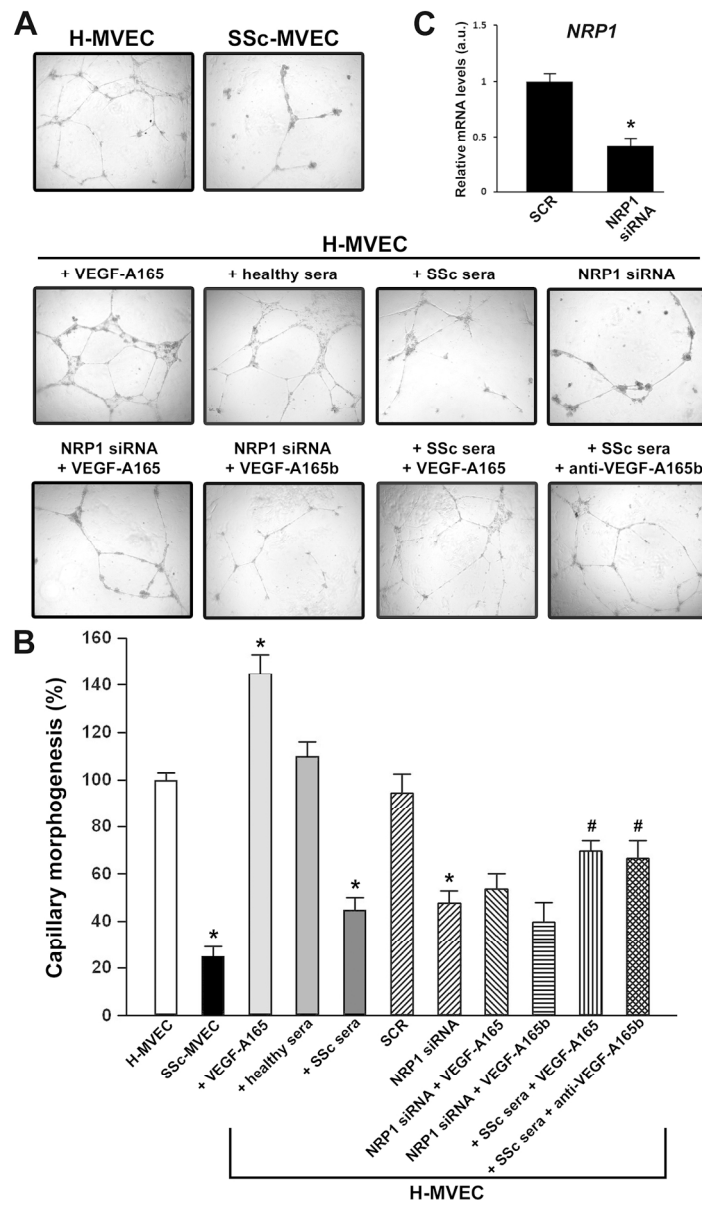
Figure 5
125x209mm (300 x 300 DPI)
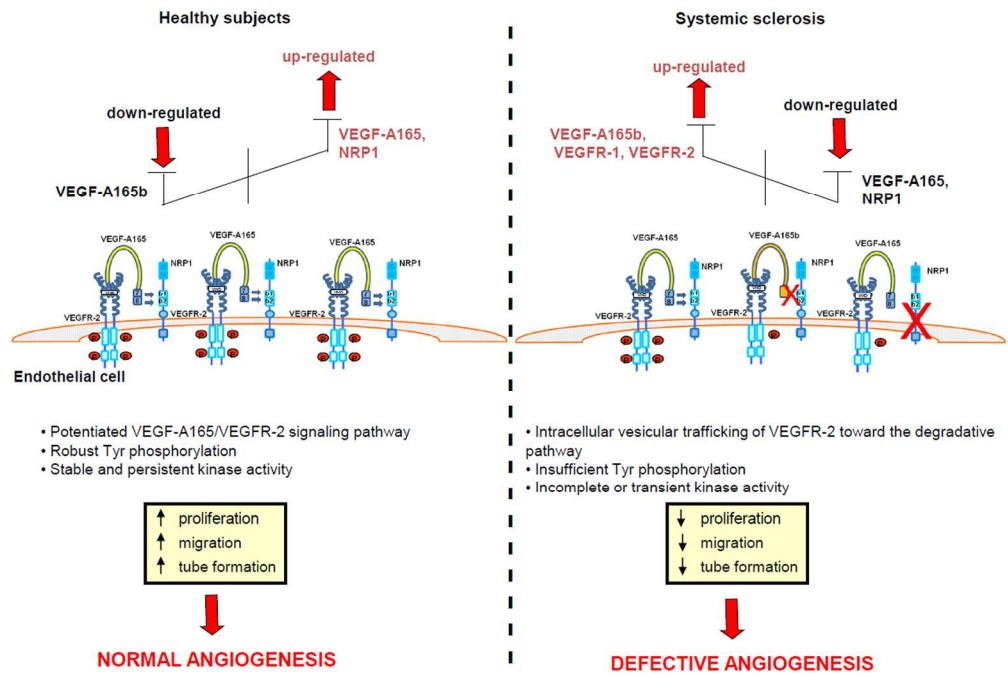
Figure 6
180x123mm (300 x 300 DPI)

Online supplementary material

METHODS

Patients, controls, serum samples and skin biopsies

Serum samples were obtained from 49 systemic sclerosis (SSc) patients [1] (45 women and 4 men; median age 64 years, range 37 to 80 years, and median disease duration 10 years, range 2 to 31 years) classified as limited cutaneous SSc (lcSSc; n = 32) or diffuse cutaneous SSc (dcSSc; n = 17) [2], and from 39 age-matched and sex-matched healthy individuals. All patients reported the occurrence of Raynaud's phenomenon. At the time blood was drawn, the presence of digital ulcers was recorded. Nailfold videocapillaroscopy (NVC) was performed on all 10 fingers by a single rheumatologist and images were scored blindly to divide patients into three capillaroscopic patterns (i.e., early, active and late) [3,4]. Clinicodemographic characteristics of SSc patients used for collection of serum samples are shown in online supplementary table S1. Patients were not on immunosuppressive medications, corticosteroids or other disease-modifying drugs. Before blood sampling, they were washed out for 10 days from oral vasodilating drugs and for 2 months from intravenous prostanoids. Fresh venous blood samples were drawn, left to clot for 30 minutes before centrifugation at $1,500\,g$ for 15 minutes, and serum was collected and stored in aliquots at −80°C until used. Full-thickness skin biopsies were obtained from the clinically involved skin of one-third of the distal forearm of 18 patients with SSc (15 women, 3 men; median age 48.5 years, range 29 to 73 years, and median disease duration 7.2 years, range 1 to 18 years). Skin samples from the same forearm region of 11 age-matched and sex-matched healthy donors were used as controls. Each skin biopsy was divided into two specimens and processed for immunohistochemistry and biomolecular analysis, respectively. For immunohistochemistry, the specimens were fixed in 10% buffered formalin, dehydrated in graded alcohol series and embedded in paraffin. For protein extraction, skin specimens were immediately immersed in liquid nitrogen and stored at −80°C until use. The study was approved by the local institutional review board at the Azienda Ospedaliero-Universitaria Careggi (AOUC), Florence, Italy, and all subjects provided written informed consent.

Isolation, culture and stimulation of dermal microvascular endothelial cells (MVECs)

Dermal MVECs were isolated from biopsies of the involved forearm skin from 5 patients with dcSSc and from 5 healthy subjects, as described elsewhere [4,5]. Patients were not taking immunosuppressive or disease-modifying drugs at the time of biopsy. Briefly, skin biopsies were

1

mechanically cleaned of epidermis and adipose tissue in order to obtain a pure specimen of vascularised dermis, and were treated as previously described [4]. Colonies of polygonal elements were detached and CD31-positive cells were subjected to immunomagnetic isolation. Isolated cells were further identified as MVECs by labelling with anti-factor VIII-related antigen and anti-CD105, followed by reprobing with anti-CD31 antibodies. MVECs were maintained in MCDB medium (Sigma-Aldrich, St Louis, Missouri, USA) supplemented with 30% fetal bovine serum (FBS), 20 μg/ml endothelial cell growth supplement (Calbiochem, Nottingham, UK), 10 μg/ml hydrocortisone, 15 IU/ml heparin, and antibiotics. MVECs from healthy subjects (H-MVECs) and SSc patients (SSc-MVECs) were used between the third and seventh passages in culture. For stimulation experiments, H-MVECs were grown to 70% confluence, and then were washed three times with serum-free medium and serum-starved overnight in MCDB medium supplemented with 2% FBS. Medium was removed and cells were incubated with 2% FBS-MCDB medium containing recombinant human vascular endothelial growth factor (VEGF)-A165 (10 ng/ml; R&D Systems, Minneapolis, Minnesota, USA), or 10% serum from SSc patients (n = 5) and healthy subjects (n = 5) for 24 hours.

Late-outgrowth peripheral blood endothelial progenitor cell (EPC)-derived endothelial cells (ECs)

Late-outgrowth EPC-derived ECs were obtained from the peripheral blood of 15 SSc patients (13 women and 2 men; n = 9 with lcSSc and n = 6 with dcSSc; median age 60 years, range 42 to 78 years) and 8 healthy individuals (all women; median age 55 years, range 30 to 65 years), as described elsewhere [5-7]. The study was approved by the local institutional review board at the Cochin Hospital, Paris, France, and all patients and control subjects provided written informed consent. Briefly, EPC isolation was performed on a 50-ml heparinised venous blood sample obtained from the forearm. Samples from hospitalised patients were obtained in the morning, at rest, during routine analysis. Patient and control samples were immediately transported to the laboratory for testing. The blood mononuclear cell fraction was collected by Ficoll density-gradient centrifugation and was resuspended in complete endothelial cell growth medium 2 (EGM-2; Lonza, Basel, Switzerland). Cells were then seeded onto separate wells of a 12-well tissue culture plate ($2x10^7$ cells/well) precoated with type I collagen (rat tail; BD Biosciences, Le Pont de Claix, France) and stored in an atmosphere of 5% CO2 at 37°C. After 24 hours of culture, non-adherent cells and debris were aspirated, adherent cells were washed once with phosphate-buffered saline (PBS), and complete EGM-2 was added to each well. The medium was changed daily for 7 days

2

and then every other day until the first passage. Colonies of ECs appeared between 8 and 26 days of culture and were identified as well-circumscribed monolayers of cells with a cobblestone appearance. After the third passage, phenotyping of EPC-derived cells was performed by flow cytometry, as previously described [6]. After confirmation of the endothelial phenotype, cells were suspended in FBS supplemented with 20% dimethyl sulfoxide, frozen in liquid nitrogen, and stored until used.

Enzyme-linked immunosorbent assay (ELISA) for serum semaphorin3A (Sema3A) and soluble neuropilin-1 (sNRP1)

The levels of Sema3A and sNRP1 in serum samples were measured by commercial quantitative colorimetric sandwich ELISA (catalogue number ABIN481720 and ABIN415191, respectively; Antibodies-on line, Atlanta, Georgia, USA) according to the manufacturer's protocol. Each sample was measured in duplicate.

Immunofluorescence

For antigen retrieval, paraffin-embedded skin sections (5 μm thick) were deparaffinised and boiled for 10 minutes in sodium citrate buffer (10 mM, pH 6.0). The sections were washed three times in PBS, incubated in 2 mg/ml glycine for 10 minutes to quench autofluorescence caused by free aldehydes, and then blocked for 1 hour at room temperature with 1% bovine serum albumin in PBS. The slides were incubated overnight at 4°C with rabbit monoclonal antihuman NRP1 antibody (1:50 dilution; catalogue number ab81321, Abcam, Cambridge, UK) or rabbit polyclonal antihuman Sema3A antibody (1:50 dilution; catalogue number ab23393, Abcam). After extensive washing in PBS, the sections were incubated with Rhodamine Red-X-conjugated goat anti-rabbit IgG (1:200 dilution; Molecular Probes, Eugene, Oregon, USA) for 45 minutes at room temperature in the dark. Irrelevant isotype-matched and concentration-matched rabbit IgG (Sigma-Aldrich) were used as negative controls. For double immunofluorescence staining, we used a mouse monoclonal antibody against CD31/pan-endothelial cell marker (1:25 dilution; catalogue number ab9498, Abcam) followed by Alexa Fluor-488-conjugated goat anti-mouse IgG (1:200 dilution; Molecular Probes). Nuclei were counterstained with 4′,6-diamidino-2-phenylindole (DAPI). The immunolabelled sections were then observed under a Leica DM4000 B microscope equipped with fully automated fluorescence axes (Leica Microsystems, Mannheim, Germany). Fluorescence images were captured using a Leica DFC310 FX 1.4-megapixel digital colour camera equipped with the Leica software application suite LAS V3.8 (Leica Microsystems).

3

Western blotting

Proteins were extracted from skin biopsies, dermal MVECs and late-outgrowth peripheral blood EPC-derived ECs as described elsewhere [7,8]. Twenty micrograms of total proteins were electrophoresed on NuPAGE 4 to 12% Bis-Tris Gel (Invitrogen, Carlsbad, California, USA) and blotted onto polyvinylidene difluoride membranes (Invitrogen). The membranes were blocked with blocking solution included in the Western Breeze Chromogenic Western Blot Immunodetection Kit (Invitrogen) for 30 minutes at room temperature on a rotary shaker and incubated for 1 hour at room temperature with rabbit monoclonal antihuman NRP1 (1:1,000 dilution; catalogue number ab81321, Abcam), rabbit polyclonal antihuman Sema3A (1:1,000 dilution; catalogue number ab23393, Abcam), rabbit polyclonal antihuman Friend leukaemia integration 1 (Fli1) (1:1,000 dilution; catalogue number ab180902, Abcam) and rabbit polyclonal anti-α-tubulin (1:1,000 dilution; catalogue number #2144, Cell Signaling Technology, Danvers, Massachusetts, USA) antibodies, assuming α-tubulin as control invariant protein. Immunodetection was performed as described in the Western Breeze Chromogenic Immunodetection protocol (Invitrogen). Densitometric analysis of the bands was performed using the free-share ImageJ software (NIH, Bethesda, Maryland, USA; online at http://rsbweb.nih.gov/ij) and the values were normalised to α-tubulin.

Gene silencing of Fli1 and NRP1

MVECs were seeded shortly before transfection. The cells were transfected with 10 nM of Fli1 small interfering RNA (siRNA), 10 nM of NRP1 siRNA or non-silencing scrambled RNA (SCR) (Santa Cruz Biotechnology, Dallas, Texas, USA) using HiPerfect transfection reagent (Qiagen, Milan, Italy) for 72 hours.

RNA purification, cDNA synthesis and quantitative real-time PCR

Total RNA was isolated from MVECs using the RNeasy Micro Kit (Qiagen). First strand cDNA was synthesised using the QuantiTect Reverse Transcription kit (Qiagen). For mRNA quantification, SYBR Green real-time PCR was performed using the StepOnePlus Real-Time PCR System (Applied Biosystems, Milan, Italy) with melting curve analysis. Predesigned oligonucleotide primer pairs were obtained from Qiagen (QuantiTect Primer Assay). The assay IDs were QT00023009 Hs_NRP1, QT00078372 Hs_FLI, and QT00199367 Hs_RRN18S. The PCR mixture contained 1 μl cDNA, 0.5 μM sense and antisense primers, 10 μl 2× QuantiTect SYBR Green PCR Master Mix containing SYBR Green I dye, ROX passive reference dye, HotStarTaq DNA Polymerase, dNTP mix and $MgCl_2$ (Qiagen). Amplification was performed according to a

4

standard protocol recommended by the manufacturer. Non-specific signals caused by primer dimers or genomic DNA were excluded by dissociation curve analysis, non-template controls and samples without enzyme in the reverse transcription step. 18S ribosomal RNA was measured as an endogenous control to normalise for the amounts of loaded cDNA. Differences were calculated with the threshold cycle (Ct) and comparative Ct method for relative quantification. All measurements were performed in triplicate.

Chromatin immunoprecipitation (ChIP) assay

The ChIP assay was carried out using EpiQuik ChIP kit (Epigentek, Farmingdale, New York, USA). Briefly, cells were treated with 1% formaldehyde for 10 minutes. The cross-linked chromatin was then prepared and sonicated to an average size of 300-500 bp. To exclude exogenous DNA contamination, negative controls were obtained by omitting the cell preparation in some specimens. The DNA fragments were immunoprecipitated with rabbit polyclonal anti-Fli1 antibody (catalogue number ab15289, Abcam) or normal rabbit IgG (catalogue number ab37415, Abcam) at 4°C. After reversal of cross-linking, the immunoprecipitated chromatin was amplified by PCR amplification of specific region of the NRP1 gene promoter. Putative Fli1 transcription factor binding site was predicted by Tfsitescan. The primers were as follows: NRP1 Forward, 5'-CTAGGGGTGCAGAGCGAG-3'; NRP1 Reverse, 5'-GAAGGAAGGCGCTGGGAG-3'. The amplified DNA products were resolved by agarose gel electrophoresis.

In vitro capillary morphogenesis assay

In vitro capillary morphogenesis assay was performed in 96-well plates covered with Matrigel (BD Biosciences). Matrigel (50 µl; 10-12 mg/ml) was pipetted into culture wells and polymerised for 30 minutes to 1 hour at 37°C. H-MVECs ($30x10^3$ cells/well) were incubated in basal MCDB medium containing 10% healthy serum (n = 5) or 10% SSc serum (n = 5), this latter used alone or in combination with recombinant human VEGF-A165 (10 ng/ml; R&D Systems), mouse monoclonal anti-human VEGF-A165b antibody (10 μg/ml; catalogue number ab14994, Abcam) or irrelevant mouse IgG. SSc-MVECs and H-MVECs transfected with NRP1 siRNA, at basal condition or challenged with recombinant human VEGF-A165 or VEGF-A165b (both 10 ng/ml; R&D Systems), or non-silencing SCR, were also assayed. Stimulation with recombinant human VEGF-A165 added to basal MCDB medium was used as positive control of angiogenesis. Plates were photographed at 6 and 24 hours. Results were quantified at 24 hours by measuring the percent field occupancy of

5

capillary projections, as determined by image analysis. Six to nine photographic fields from 3 plates were scanned for each experimental point.

Statistical analysis

Statistical analyses were performed using the Statistical Package for Social Sciences (SPSS) software for Windows, version 20.0 (SPSS, Chicago, Illinois, USA). Data are expressed as mean ± SD or median and interquartile range (IQR). The Student's *t*-test and nonparametric Mann-Whitney *U*-test were used where appropriate for statistical evaluation of the differences between two independent groups. A p-value less than 0.05 was considered statistically significant.

REFERENCES

1) van den Hoogen F, Khanna D, Fransen J, *et al*. 2013 classification criteria for systemic sclerosis: an American College of Rheumatology/European League against Rheumatism collaborative initiative. *Ann Rheum Dis* 2013;72:1747-55.

2) LeRoy EC, Black C, Fleischmajer R, *et al*. Scleroderma (systemic sclerosis): classification, subsets, and pathogenesis. *J Rheumatol* 1988;15:202-5.

3) Manetti M, Guiducci S, Romano E, *et al*. Increased serum levels and tissue expression of matrix metalloproteinase-12 in patients with systemic sclerosis: correlation with severity of skin and pulmonary fibrosis and vascular damage. *Ann Rheum Dis* 2012;71:1064-72.

4) Manetti M, Guiducci S, Romano E, *et al*. Differential expression of junctional adhesion molecules in different stages of systemic sclerosis. Arthritis Rheum 2013;65:247-57.

5) Manetti M, Guiducci S, Romano E, *et al*. Decreased expression of the endothelial cell-derived factor EGFL7 in systemic sclerosis: potential contribution to impaired angiogenesis and vasculogenesis. *Arthritis Res Ther* 2013;15:R165.

6) Avouac J, Wipff J, Goldman O, *et al*. Angiogenesis in systemic sclerosis: impaired expression of vascular endothelial growth factor receptor 1 in endothelial progenitor-derived cells under hypoxic conditions. *Arthritis Rheum* 2008;58:3550-61.

7) Avouac J, Cagnard N, Distler JH, *et al*. Insights into the pathogenesis of systemic sclerosis based on the gene expression profile of progenitor-derived endothelial cells. *Arthritis Rheum* 2011;63:3552-62.

8) Manetti M, Guiducci S, Romano E, *et al*. Overexpression of VEGF165b, an inhibitory splice variant of vascular endothelial growth factor, leads to insufficient angiogenesis in patients with systemic sclerosis. *Circ Res* 2011;109:e14-26.

6

Supplementary Table S1. Demographic and clinical characteristics of the 49 patients with systemic sclerosis (SSc) included for collection of serum samples.

Characteristics	SSc patients
Age, years, median (range)	64 (37 to 80)
Sex	
Male	4 (8)
Female	45 (92)
Disease subset	
lcSSc	32 (65)
dcSSc	17 (35)
Disease duration, years, median (range)[a]	10 (2 to 31)
Autoantibody positivity	
ANA	49 (100)
ACA	32 (65)
Anti-topo I	11 (22)
Digital ulcers	27 (55)
Digital pitting scars	15 (31)
Nailfold videocapillaroscopy pattern	
Early	11 (22)
Active	21 (43)
Late	17 (35)
Skin score, median (range)[b]	6 (0 to 35)
Interstitial lung disease[c]	27 (55)
2013 ACR/EULAR score, median (range)	14 (10 to 28)

Except where indicated otherwise, values are the number (%) of subjects.
[a]Disease duration was calculated since the first non-Raynaud's symptom of SSc; [b]modified Rodnan skin thickness score; [c]Determined by thoracic high-resolution computer tomography. ACA, anticentromere antibodies; ACR, American College of Rheumatology; ANA, antinuclear antibodies; Anti-topo I, anti-topoisomerase I antibodies; dcSSc, diffuse cutaneous SSc; EULAR, European League Against Rheumatism; lcSSc, limited cutaneous SSc.

7

Decreased expression of neuropilin-1 as a novel key factor contributing to peripheral microvasculopathy and defective angiogenesis in systemic sclerosis

Eloisa Romano[1#*], Inês Chora[1,2#], Mirko Manetti[3#], Celestina Mazzotta[1], Irene Rosa[1,3], Silvia Bellando-Randone[1], Jelena Blagojevic[1], Raquel Soares[4], Jerôme Avouac[5], Yannick Allanore[5], Lidia Ibba-Manneschi[3], Marco Matucci-Cerinic[1], Serena Guiducci[1]

[1]Department of Experimental and Clinical Medicine, Division of Rheumatology, Azienda Ospedaliero-Universitaria Careggi (AOUC), University of Florence, Florence, Italy

[2]Department of Internal Medicine, São João Hospital Center, Al Prof Hernâni Monteiro, Porto, Portugal

[3]Department of Experimental and Clinical Medicine, Section of Anatomy and Histology, University of Florence, Florence, Italy

[4]Department of Biochemistry, Faculty of Medicine, University of Porto, Al Prof Hernâni Monteiro, Porto, Portugal

[5]Cochin Institute, Paris Descartes University, INSERM U1016 and CNRS UMR8104, Paris, France

*Correspondence to:

Eloisa Romano,
Department of Experimental and Clinical Medicine,
Division of Rheumatology,
University of Florence,
Viale Pieraccini 6,
50139 Florence, Italy
Email: eloisaromano@libero.it

[#]Eloisa Romano, Inês Chora and Mirko Manetti contributed equally to this work.

1

ABSTRACT

Objectives: In systemic sclerosis (SSc), vascular involvement is characterised by VEGF-A/VEGFR system disturbances. Neuropilin-1 (NRP1), a receptor for both class-3 semaphorins (Sema3s) and VEGF-A, is required for optimal VEGF-A/VEGFR-2 signalling. Here, we investigated the possible involvement of Sema3A/NRP1 axis in SSc.

Methods: Circulating Sema3A and soluble NRP1 (sNRP1) were measured in SSc patients and controls. NRP1 and Sema3A expression in skin biopsies was evaluated by immunofluorescence and Western blotting. NRP1 expression was assessed in SSc and healthy dermal microvascular endothelial cells (SSc-MVECs and H-MVECs), and in SSc and control endothelial progenitor cell (EPC)-derived ECs. The possible impact of transcription factor Fli1 deficiency on endothelial NRP1 expression was investigated by gene silencing. The binding of Fli1 to NRP1 gene promoter was evaluated using chromatin immunoprecipitation. Capillary morphogenesis was performed on Matrigel.

Results: Decreased sNRP1 levels in SSc were associated with active and late nailfold videocapillaroscopy patterns and digital ulcers. No difference in Sema3A was found between patients and controls. NRP1 was significantly decreased in SSc-MVECs both *ex vivo* and *in vitro*. NRP1 and Fli1 significantly decreased in H-MVECs challenged with SSc sera, while they were not different in SSc and control EPC-derived ECs. Fli1 occupied the NRP1 gene promoter and Fli1 gene silencing reduced NRP1 expression in H-MVECs. NRP1 gene silencing in H-MVECs resulted in a significantly impaired angiogenic capacity comparable to that of cells treated with SSc sera.

Conclusions: In SSc, NRP1 deficiency may be an additional factor in the perturbed VEGF-A/VEGFR-2 system contributing to peripheral microvasculopathy and defective angiogenesis.

Keywords: systemic sclerosis, neuropilin-1, Fli1, dermal microvascular endothelial cells, angiogenesis, peripheral microvasculopathy

2

INTRODUCTION

Systemic sclerosis (SSc, scleroderma) is a life-threatening connective tissue disorder of unknown aetiology, characterised by widespread vascular injury and dysfunction, impaired angiogenesis, immune dysregulation and progressive fibrosis of the skin and internal organs [1,2]. The dysregulation of vascular tone control, clinically evident as Raynaud's phenomenon, and microcirculatory abnormalities paralleled by nailfold capillaroscopic changes are the earliest clinical manifestations of SSc and may precede skin and visceral involvement by months or years [1-3]. The whole process is characterised by an uncontrolled regeneration of the microvasculature and subsequent loss of microvessels, due to defects in both vascular repair and expected increase in new vessel growth (angiogenesis), leading to severe peripheral ischaemic manifestations, such as digital ulcers and gangrene [2,3].

Recent studies have highlighted the anatomic and structural similarities between blood vessels and nerves [4]. The two networks are often aligned, with nerve fibers and blood vessels following parallel routes. Furthermore, both systems require precise control over their guidance and growth. Several molecules with attractive and repulsive properties have been found to modulate the guidance both of nerves and blood vessels [4]. These include the neuropilin receptors and their semaphorin ligands, as well as netrins, slits and their receptors [4]. Among these, neuropilin-1 (NRP1) was initially described as an axonally expressed receptor for secreted class-3 semaphorins (Sema3s), a family of soluble molecules which modulate the development of the nervous and vascular systems [5,6]. NRP1 also serves as specific vascular endothelial growth factor-A (VEGF-A) co-receptor on endothelial cells (ECs) and regulates VEGF receptor (VEGFR) signalling, leading to enhanced migration [7] and survival of ECs *in vitro* [8,9]. Furthermore, NRP1 has been implicated in VEGFR-2-mediated endothelial permeability [10] and in VEGF-A-induced three-dimensional EC biology, such as vessel sprouting and branching [11]. The absence of functional NRP1 in mice results in embryonic death due to impaired heart and blood vessel development, thus suggesting that this receptor plays a central regulatory role during developmental angiogenesis [4]. The exact molecular mechanisms by which NRP1 modulates VEGF-A biology remain to be elucidated. It has, however, been shown that NRP1 potentiates the VEGF-A/VEGFR-2 signalling pathways implicated in the migratory response of ECs [12].

The evidence that NRP1 functions as a receptor for both VEGF-A and Sema3s suggests that these latter may also play a role in the modulation of angiogenesis. In particular, it has been reported that Sema3A acts as an antiangiogenic molecule impairing EC adhesion, migration and survival *in vitro* [13-15], and regulates tumour-induced angiogenesis *in vivo* [16]. Moreover, Sema3A null mice

3

exhibit defects in blood vessel reshaping [15,17,18]. The molecular mechanisms underlying the antiangiogenic effects of Sema3A are complex. Hence, it was initially suggested that Sema3A competes with VEGF-A for NRP1 binding, thus inhibiting VEGF-A-induced angiogenesis. However, recent reports have also shown that Sema3A increases vascular permeability, inhibits EC proliferation, and induces apoptosis even in the absence of VEGF-A, suggesting that Sema3A may activate its own signalling pathways [19,20].

On these bases, we hypothesised that the Sema3A/NRP1 axis might play a role in the pathogenesis of SSc-related microvascular abnormalities. Therefore, the aim of the present study was to investigate whether the levels of Sema3A and NRP1 could be altered in the circulation, skin and ECs of SSc patients, as well as the mechanism explaining the dysregulated expression of these molecules and their possible contribution to the disturbed angiogenesis of SSc.

METHODS

An extended methods section is provided in the online supplementary material.

Patients, controls, serum samples and skin biopsies

Serum samples were obtained from 49 SSc patients [1] (45 women and 4 men; median age 64 years, range 37 to 80 years, and median disease duration 10 years, range 2 to 31 years) classified as limited cutaneous SSc (lcSSc; n = 32) or diffuse cutaneous SSc (dcSSc; n = 17) [21], and from 39 age-matched and sex-matched healthy individuals. All patients were clinically assessed as described elsewhere [3,22,23]. Clinicodemographic characteristics of SSc patients used for collection of serum samples are shown in online supplementary table S1. Full-thickness skin biopsies were obtained from the clinically involved skin of one-third of the distal forearm of 18 patients with SSc (15 women, 3 men; median age 48.5 years, range 29 to 73 years, and median disease duration 7.2 years, range 1 to 18 years). Skin samples from the same forearm region of 11 age-matched and sex-matched healthy donors were used as controls. Each skin biopsy was divided into two specimens and processed for immunohistochemistry and biomolecular analysis as described elsewhere [23]. The study was approved by the local institutional review board at the Azienda Ospedaliero-Universitaria Careggi (AOUC), Florence, Italy, and all subjects provided written informed consent.

Isolation, culture and stimulation of dermal microvascular endothelial cells (MVECs)

Dermal MVECs were isolated from biopsies of the involved forearm skin from 5 patients with dcSSc and from 5 healthy subjects, as described elsewhere [3,23]. MVECs from healthy subjects (H-MVECs) and SSc patients (SSc-MVECs) were used between the third and seventh passages in culture. For stimulation experiments, H-MVECs were grown to 70% confluence, and then were washed three times with serum-free medium and serum-starved overnight in MCDB medium supplemented with 2% FBS. Medium was removed and cells were incubated with 2% FBS-MCDB medium containing recombinant human VEGF-A165 (10 ng/ml; R&D Systems, Minneapolis, Minnesota, USA), or 10% serum from SSc patients (n = 5) and healthy subjects (n = 5) for 24 hours.

Late-outgrowth peripheral blood endothelial progenitor cell (EPC)-derived ECs

Late-outgrowth EPC-derived ECs were obtained from the peripheral blood of 15 SSc patients (13 women and 2 men; n = 9 with lcSSc and n = 6 with dcSSc; median age 60 years, range 42 to 78 years) and 8 healthy individuals (all women; median age 55 years, range 30 to 65 years), as described elsewhere [3,24,25].

Enzyme-linked immunosorbent assay (ELISA) for serum Sema3A and soluble NRP1 (sNRP1)

The levels of Sema3A and sNRP1 in serum samples were measured by commercial quantitative colorimetric sandwich ELISA (catalogue number ABIN481720 and ABIN415191, respectively; Antibodies-on line, Atlanta, Georgia, USA) according to the manufacturer's protocol. Each sample was measured in duplicate.

Immunofluorescence

Immunofluorescence on paraffin-embedded skin sections was performed as previously described [3]. For primary and secondary antibodies, refer to the online supplementary material.

Western blotting

Proteins were extracted from skin biopsies, dermal MVECs and late-outgrowth peripheral blood EPC-derived ECs as described elsewhere [3,25,26]. Western blotting was carried out according to previously published protocols [3]. For primary antibodies, refer to the online supplementary material.

5

Gene silencing of Friend leukaemia integration 1 (Fli1) and NRP1

MVECs were seeded shortly before transfection. The cells were transfected with 10 nM of Fli1 small interfering RNA (siRNA), 10 nM of NRP1 siRNA or non-silencing scrambled RNA (SCR) (Santa Cruz Biotechnology, Dallas, Texas, USA) using HiPerfect transfection reagent (Qiagen, Milan, Italy) for 72 hours.

RNA purification, cDNA synthesis and quantitative real-time PCR

Total RNA isolation from MVECs, first strand cDNA synthesis and mRNA quantification by SYBR Green real-time PCR was performed as reported elsewhere [27]. For predesigned oligonucleotide primer pairs obtained from Qiagen, refer to the online supplementary material.

Chromatin immunoprecipitation (ChIP) assay

The ChIP assay was carried out as previously described [28] using a rabbit polyclonal anti-Fli1 antibody (catalogue number ab15289, Abcam, Cambridge, UK). Putative Fli1 transcription factor binding site was predicted by Tfsitescan. The primers were as follows: NRP1 Forward, 5'-CTAGGGGTGCAGAGCGAG-3'; NRP1 Reverse, 5'-GAAGGAAGGCGCTGGGAG-3'.

In vitro capillary morphogenesis assay

In vitro capillary morphogenesis assay on Matrigel was performed according to previously published protocols [27] as detailed in the online supplementary material.

Statistical analysis

Statistical analyses were performed using the Statistical Package for Social Sciences (SPSS) software for Windows, version 20.0 (SPSS, Chicago, Illinois, USA). Data are expressed as mean$\pm$SD or median and interquartile range (IQR). The Student's *t*-test and nonparametric Mann-Whitney *U*-test were used where appropriate for statistical evaluation of the differences between two independent groups. A p-value less than 0.05 was considered statistically significant.

RESULTS

Serum Sema3A and sNRP1 levels in SSc

No significant differences in serum levels of Sema3A were detected between SSc patients (median 2.22 ng/ml, IQR 1.84 to 3.17 ng/ml) and healthy controls (median 3.86 ng/ml, IQR 1.64 to 4.73

6

ng/ml) (figure 1A). Circulating sNRP1 levels were significantly reduced in SSc patients (median 0.22 ng/ml, IQR 0.0 to 0.6 ng/ml) compared with healthy individuals (median 0.69 ng/ml, IQR 0.0 to 2.5 ng/ml; p=0.001) (figure 1B). Next, we evaluated the possible correlation of serum sNRP1 levels with the nailfold videocapillaroscopy (NVC) pattern as a measure of peripheral microvascular involvement. sNRP1 levels were significantly decreased either in SSc patients with active (median 0.14 ng/ml, IQR 0.0 to 0.4 ng/ml) or late (median 0.09 ng/ml, IQR 0.0 to 0.72 ng/ml) NVC patterns than in controls (p=0.003 and p=0.01, respectively) (figure 1C). Conversely, no difference in serum sNRP1 was found between SSc patients with early NVC pattern (median 0.45 ng/ml, IQR 0.22 to 0.66 ng/ml) and healthy controls (figure 1C). Moreover, sNRP1 levels were significantly decreased in SSc patients with digital ulcers (median 0.06 ng/ml, IQR 0.0 to 0.27 ng/ml) compared both with patients without digital ulcers (median 0.43 ng/ml, IQR 0.17 to 0.71 ng/ml; p=0.009) and controls (p=0.001) (figure 1D). No significant association was found with other clinicodemographic and laboratory parameters or with clinical SSc subset.

Decreased expression of NRP1 in SSc dermal ECs *ex vivo* and *in vitro*

The expression of Sema3A and NRP1 protein in forearm skin biopsies from SSc patients and controls was investigated by immunofluorescence and Western blot. No significant differences in Sema3A expression were detected between SSc and control skin (figure 2A-C). On the contrary, NRP1 expression was decreased in clinically affected skin biopsies from SSc patients compared to healthy skin, in particular in dermal ECs and perivascular stromal cells (figure 3A-F). The localisation of NRP1 staining in vascular ECs was confirmed by NRP1/CD31 double immunofluorescence staining (figure 3C,F). Moreover, Western blot analysis confirmed that NRP1 protein expression levels were significantly reduced in SSc skin in respect to control skin (p<0.001) (figure 3G,H).

Western blot analysis on cultured dermal MVECs revealed that NRP1 protein expression levels were significantly reduced in SSc-MVECs compared to H-MVECs (p<0.005) (figure 4A). Moreover, NRP1 expression in H-MVECs significantly increased after treatment with healthy sera compared to basal condition, while it decreased after challenging with SSc sera (both p<0.005 *vs* basal H-MVECs). As expected, stimulation with recombinant human VEGF-A165 strongly upregulated NRP1 expression in H-MVECs (p<0.005 *vs* basal H-MVECs) (figure 4A). On the contrary, no obvious differences in NRP1 protein levels could be found between late-outgrowth EPC-derived ECs from SSc patients and healthy controls (figure 4B).

7

Fli1 deficiency contributes to the downregulation of NRP1 gene in SSc-MVECs

We next examined the potential mechanism by which NRP1 expression is downregulated in dermal SSc microvessels. As the expression of the transcription factor Fli1 is markedly downregulated at least partially *via* an epigenetic mechanism in SSc dermal ECs, and experimental endothelial Fli1 deficiency reproduces the histopathological and functional abnormalities characteristic of SSc vasculopathy [28-30], we hypothesised that endothelial Fli1 deficiency could inhibit the expression of NRP1 in SSc-MVECs.

First, we analysed Fli1 protein expression in cultured dermal MVECs and late-outgrowth EPC-derived ECs from SSc patients and controls (figure 4C,D). As shown in figure 4C, Fli1 protein expression in H-MVECs closely paralleled that of NRP1 in the different experimental conditions assayed, and was strongly downregulated in SSc-MVECs. Similarly to what observed for NRP1 expression, Fli1 protein levels did not differ between SSc and control late-outgrowth EPC-derived ECs (figure 4D).

Moreover, we examined the effect of Fli1 gene silencing on mRNA levels of the NRP1 gene in H-MVECs. As displayed in figure 4E, gene silencing of Fli1 significantly suppressed the mRNA expression levels of the NRP1 gene in H-MVECs (p<0.01). In addition, ChIP analysis revealed that Fli1 occupied the promoter region of the NRP1 gene in H-MVECs (figure 4F). These results indicate that Fli1 directly targets the NRP1 gene promoter and is required for homeostatic NRP1 expression in ECs.

NRP1 deficiency contributes to the impaired angiogenesis of SSc-MVECs

To verify whether endothelial NRP1 deficiency has a role in the modulation of angiogenesis, we carried out *in vitro* capillary morphogenesis on Matrigel matrix. Consistent with previous findings [26], capillary morphogenesis was significantly impaired in SSc-MVECs compared with H-MVECs (p<0.01) (figure 5). H-MVECs stimulated with healthy sera produced an abundant network of branching cords (figure 5). On the contrary, as previously reported [31,32] angiogenesis was significantly reduced upon challenge with SSc sera (p<0.01 *vs* basal H-MVECs) (figure 5). The addition of recombinant human VEGF-A165 or anti-VEGF-A165b blocking antibodies to SSc sera significantly increased H-MVEC angiogenesis compared with cells treated with SSc sera alone (both p<0.05) (figure 5). NRP1 gene silencing in H-MVECs resulted in a significant impairment of angiogenic capacity comparable to that of cells treated with SSc sera (p<0.01 *vs* basal H-MVECs) (figure 5). Stimulation of NRP1-silenced H-MVECs with recombinant human proangiogenic

8

VEGF-A165 or antiangiogenic VEGF-A165b could only slightly increase or decrease angiogenesis, respectively (figure 5).

DISCUSSION

Here, we investigated for the first time the possible involvement of the Sema3A/NRP1 axis in the pathogenesis of SSc. Our present findings clearly demonstrate that serum levels and dermal expression of NRP1 are significantly decreased in SSc patients and that lower circulating sNRP1 levels correlate with the severity of NVC abnormalities and the presence of digital ulcers. In contrast to constitutive endothelial expression of NRP1 in healthy skin, NRP1 was found to be strongly reduced *ex vivo* in SSc dermal microvessels, and NRP1 downregulation was maintained *in vitro* in MVECs obtained from SSc dermis. On the contrary, we could not find any difference in NRP1 protein levels between peripheral blood EPC-derived ECs from SSc patients and healthy controls. This evidence suggests that the dysregulated expression of this receptor is restricted to locally injured microvasculature in an overt disease without affecting bone marrow-derived circulating endothelial progenitors. As far as Sema3A is concerned, no difference in its expression was observed between SSc and controls either in the circulation or in the cutaneous tissue.

The importance of NRP1 for vascular development is well established and shown by the generation of knockout mice, which display an embryonic lethal phenotype characterised by severe vascular defects due to impaired angiogenic sprouting and branching very much resembling the disturbed vessel morphology seen in SSc patients [4,33,34]. Moreover, conditional NRP1 knockout in ECs is associated with important cardiac and vascular defects, thus suggesting a crucial role for NRP1 in EC functions [35]. Even though NRP1 was originally identified as an adhesion molecule in the nervous system, it is more commonly studied as receptor for the neuronal guidance molecule Sema3A and as co-receptor for the VEGF-A165/VEGFR-2 complex with key roles in neuronal and vascular development [12,36]. Of note, several studies have implicated a dysfunctional VEGF-A/VEGFR-2 system in the impaired angiogenic process characteristic of SSc [2,26,37-39]. Moreover, besides VEGF-A, it is well known that a dysregulated expression of a large array of proangiogenic and antiangiogenic (angiostatic) factors present in the circulation of SSc patients may be mostly responsible for such angiogenic deficit [2,37-40].

In our study, not only we observed that the proangiogenic NRP1 receptor was constitutively downregulated in dermal SSc-MVECs, but also that treatment with SSc sera could significantly reduce NRP1 expression in H-MVECs, which is in line with the reported antiangiogenic properties

9

of SSc sera [2,31,32,37,41]. Strikingly, we also found that NRP1 gene silencing in H-MVECs resulted in a significantly impaired angiogenic process comparable to that of cells treated with SSc sera, further supporting the implication of NRP1 deficiency in the disturbed angiogenesis of SSc. Consistent with previous studies, stimulation with recombinant proangiogenic VEGF-A165 strongly upregulated NRP1 expression in H-MVECs suggesting that this growth factor cannot only activate ECs directly, but can also contribute to angiogenesis by a mechanism that involves upregulation of its homologous receptor NRP1 [36]. The findings of NRP1 downregulation in H-MVECs upon challenge with SSc sera are in agreement with the evidence that the majority of VEGF-A detected in SSc circulation is not the proangiogenic VEGF-A165, but rather the antiangiogenic VEGF-A165b isoform [26,42]. Further, it has been reported that VEGF-A165b is unable to bind the co-receptor NRP1 because the basic carboxyterminal amino acids essential for NRP1 binding are absent in this splice variant [43,44]. Interestingly, we observed that stimulation of H-MVECs silenced for the NRP1 co-receptor with proangiogenic VEGF-A165 slightly increased angiogenesis, while stimulation with VEGF-A165b isoform resulted only in a slight decrease in their angiogenic capacity. These data are consistent with the antiangiogenic action of VEGF-A165b being mainly dependent on its inability to recruit VEGFR-2/NRP1 co-receptor complex and activate downstream signalling. In a recent study, it was demonstrated that VEGF-A165 and VEGF-A165b may control the balance between VEGFR-2 recycling, degradation and signalling. In particular, due to the lack of NRP1 co-receptor binding, VEGF-A165b may induce differential intracellular vesicular trafficking of VEGFR-2 toward the degradative pathway [45]. Thus, both a switch from the proangiogenic to the antiangiogenic VEGF-A isoform and the concomitant NRP1 co-receptor downregulation may have a crucial role in the insufficient angiogenic response found in SSc (figure 6). Indeed, here we also demonstrated that both the addition of recombinant human VEGF-A165 or anti-VEGF-A165b blocking antibodies could significantly dampen the antiangiogenic effects of SSc sera on H-MVECs.

The clinical correlation of serum sNRP1 levels with the severity of SSc-related peripheral microvasculopathy also deserves discussion. Indeed, circulating levels of sNRP1 progressively decreased reaching the lowest values in SSc patients with the active and late NVC patterns, which are characterised by severe architectural changes of microvessels and progressive capillary loss with formation of avascular areas [46]. In addition, patients with active/late NVC patterns and digital ulcers showed serum sNRP1 levels significantly lower than healthy controls, whereas sNRP1 levels did not differ significantly between controls and SSc patients with early NVC pattern and lack of digital ulcers. However, since sNRP1 may be largely released by ECs, we should also consider that

10

the reduction in circulating levels of sNRP1 might be either a cause or a consequence of the disease, which is characterised by progressive loss of the peripheral microcirculation [2,3,46]. Circulating levels of sNRP1 could even serve as a biomarker reflecting the severity and progression of SSc microvasculopathy. Accordingly, further prospective studies on larger cohorts of SSc patients are warranted.

Finally, our mechanistic findings indicate that in SSc, endothelial NRP1 expression is suppressed at least partially due to Fli1 transcription factor deficiency. In fact, here we provide the first evidence that NRP1 is a member of the angiogenesis-related gene program regulated by Fli1 in dermal MVECs. In this context, the impact of Fli1 deficiency in the loss of EC integrity and the development of peripheral microvasculopathy during SSc has been well established [28-30]. Of note, it has been demonstrated that in SSc Fli1 expression is markedly suppressed at least partially through an epigenetic mechanism [29,30]. Thus, such an epigenetic modification might partly explain the persistence of the multiple downstream effects of Fli1 deficiency in an *in vitro* culture system, as supported by the downregulation of endothelial NRP1 observed *ex vivo* in SSc dermal microvessels and maintained in cultured dermal SSc-MVECs. Interestingly, NRP1 was found to be also a target of the antiangiogenic microRNA miR-320, and a dysregulated microRNA profile is being increasingly reported in SSc [47,48].

In conclusion, we shed light on NRP1 deficiency as a novel key factor contributing to peripheral microvasculopathy and defective angiogenesis in SSc. Further studies are warranted to decipher whether therapeutic modulation of VEGF-A/VEGFR-2/NRP1 co-receptor signalling might pave the way to boost angiogenesis and block the progression of peripheral microvasculopathy in SSc.

11

Competing interests
None declared.

REFERENCES

1) van den Hoogen F, Khanna D, Fransen J, *et al*. 2013 classification criteria for systemic sclerosis: an American College of Rheumatology/European League against Rheumatism collaborative initiative. *Ann Rheum Dis* 2013;72:1747-55.

2) Manetti M, Guiducci S, Ibba-Manneschi L, *et al*. Mechanisms in the loss of capillaries in systemic sclerosis: angiogenesis versus vasculogenesis. *J Cell Mol Med* 2010;14:1241-54.

3) Manetti M, Guiducci S, Romano E, *et al*. Decreased expression of the endothelial cell-derived factor EGFL7 in systemic sclerosis: potential contribution to impaired angiogenesis and vasculogenesis. *Arthritis Res Ther* 2013;15:R165.

4) Larrivée B, Freitas C, Suchting S, *et al*. Guidance of vascular development: lessons from the nervous system. *Circ Res* 2009;104:428-41.

5) He Z, Tessier-Lavigne M. Neuropilin is a receptor for the axonal chemorepellent Semaphorin III. *Cell* 1997;90:739-51.

6) Kolodkin AL, Levengood DV, Rowe EG, *et al*. Neuropilin is a semaphorin III receptor. *Cell* 1997;90:753-62.

7) Vander Kool CW, Jusino MA, Perman B, *et al*. Structural basis for ligand and heparin binding to neuropilin B domains. *Proc Natl Acad Sci USA* 2007;104:6152-7.

8) Favier B, Alam A, Barron P, *et al*. Neuropilin-2 interacts with VEGFR-2 and VEGFR-3 and promotes human endothelial cell survival and migration. *Blood* 2006;108:1243-50.

9) Wang L, Zeng H, Wang P, *et al*. Neuropilin-1-mediated vascular permeability factor/vascular endothelial growth factor-dependent endothelial cell migration. *J Biol Chem* 2003;278:48848-60.

10) Becker PM, Waltenberger J, Yachechko R, *et al*. Neuropilin-1 regulates vascular endothelial growth factor-mediated endothelial permeability. *Circ Res* 2005;96:1257-65.

11) Kawamura H, Li X, Goishi K, *et al*. Neuropilin-1 in regulation of VEGF-induced activation of p38MAPK and endothelial cell organization. *Blood* 2008;112:3638-49.

12) Koch S. Neuropilin signaling in angiogenesis. *Biochem Soc Trans* 2012;40:20-5.

13) Miao HQ, Soker S, Feiner L, *et al*. Neuropilin-1 mediates collapsin-1/semaphorin III inhibition of endothelial cell motility: functional competition of collapsin-1 and vascular endothelial growth factor-165. *J Cell Biol* 1999;146:233-42.

12

14) Guttmann-Raviv N, Shraga-Heled N, Varshavsky A, *et al.* Semaphorin-3A and semaphorin-3F work together to repel endothelial cells and to inhibit their survival by induction of apoptosis. *J Biol Chem* 2007;282:26294-305.

15) Serini G, Valdembri D, Zanivan S, *et al.* Class 3 semaphorins control vascular morphogenesis by inhibiting integrin function. *Nature* 2003;424:391-7.

16) Maione F, Molla F, Meda C, *et al.* Semaphorin 3A is an endogenous angiogenesis inhibitor that blocks tumor growth and normalizes tumor vasculature in transgenic mouse models. *J Clin Invest* 2009;119:3356-72.

17) Gu C, Rodriguez ER, Reimert DV, *et al.* Neuropilin-1 conveys semaphorin and VEGF signaling during neural and cardiovascular development. *Dev Cell* 2003;5:45-57.

18) Arese M, Serini G, Bussolino F. Nervous vascular parallels: axon guidance and beyond. *Int J Dev Biol* 2011;55:439-45.

19) Appleton BA, Wu P, Maloney J, *et al.* Structural studies of neuropilin/antibody complexes provide insights into semaphoring and VEGF binding. *EMBO J* 2007;26:4902-12.

20) Sakurai A, Doçi CL, Gutkind JS. Semaphorin signaling in angiogenesis, lymphangiogenesis and cancer. *Cell Res* 2012;22:23-32.

21) LeRoy EC, Black C, Fleischmajer R, *et al.* Scleroderma (systemic sclerosis): classification, subsets, and pathogenesis. *J Rheumatol* 1988;15:202-5.

22) Manetti M, Guiducci S, Romano E, *et al.* Increased serum levels and tissue expression of matrix metalloproteinase-12 in patients with systemic sclerosis: correlation with severity of skin and pulmonary fibrosis and vascular damage. *Ann Rheum Dis* 2012;71:1064-72.

23) Manetti M, Guiducci S, Romano E, *et al.* Differential expression of junctional adhesion molecules in different stages of systemic sclerosis. Arthritis Rheum 2013;65:247-57.

24) Avouac J, Wipff J, Goldman O, *et al.* Angiogenesis in systemic sclerosis: impaired expression of vascular endothelial growth factor receptor 1 in endothelial progenitor-derived cells under hypoxic conditions. *Arthritis Rheum* 2008;58:3550-61.

25) Avouac J, Cagnard N, Distler JH, *et al.* Insights into the pathogenesis of systemic sclerosis based on the gene expression profile of progenitor-derived endothelial cells. *Arthritis Rheum* 2011;63:3552-62.

26) Manetti M, Guiducci S, Romano E, *et al.* Overexpression of VEGF165b, an inhibitory splice variant of vascular endothelial growth factor, leads to insufficient angiogenesis in patients with systemic sclerosis. *Circ Res* 2011;109:e14-26.

27) Guiducci S, Manetti M, Romano E, *et al.* Bone marrow-derived mesenchymal stem cells from early diffuse systemic sclerosis exhibit a paracrine machinery and stimulate angiogenesis in vitro. *Ann Rheum Dis* 2011;70:2011-21.

28) Saigusa R, Asano Y, Taniguchi T, *et al.* A possible contribution of endothelial CCN1 downregulation due to Fli1 deficiency to the development of digital ulcers in systemic sclerosis. *Exp Dermatol* 2015;24:127-32.

29) Manetti M, Fli1 deficiency and beyond: a unique pathway linking peripheral vasculopathy and dermal fibrosis in systemic sclerosis. *Exp Dermatol* 2015;24:256-57.

30) Asano Y, Bujor AM, Trojanowska M, The impact of Fli1 deficiency on the pathogenesis of systemic sclerosis. *J Dermatol Sci* 2010;59:153-62.

13

31) Romano E, Bellando-Randone S, Manetti M, *et al.* Bosentan blocks the antiangiogenic effects of sera from systemic sclerosis patients: an in vitro study. *Clin Exp Rheumatol* 2015 Jun 19. [Epub ahead of print]

32) Borghini A, Manetti M, Nacci F, *et al.* Systemic sclerosis sera impair angiogenic performance of dermal microvascular endothelial cells: therapeutic implications of cyclophosphamide. *PLoS One* 2015;10:e0130166.

33) Kitsukawa T, Shimizu M, Sanbo M, *et al.* Neuropilin-semaphorin III/D-mediated chemorepulsive signals play a crucial role in peripheral nerve projection in mice. *Neuron* 1997;19:995-1005.

34) Kawasaki T, Kitsukawa T, Bekku Y, *et al.* A requirement for neuropilin-1 in embryonic vessel formation. *Development* 1999;126:4895-902.

35) Mukouyama YS, Gerber HP, Ferrara N, *et al.* Peripheral nerve-derived VEGF promotes arterial differentiation via neuropilin 1-mediated positive feedback. *Development* 2005;32:941-52.

36) Oh H, Takagi H, Otani A, *et al.* Selective induction of neuropilin-1 by vascular endothelial growth factor (VEGF): a mechanism contributing to VEGF-induced angiogenesis. *Proc Natl Acad Sci USA* 2002;99:383-8.

37) Matucci-Cerinic M, Kahaleh B, Wigley FM. Review: evidence that systemic sclerosis is a vascular disease. *Arthritis Rheum* 2013;65:1953-62.

38) Manetti M, Guiducci S, Ibba-Manneschi L, *et al.* Impaired angiogenesis in systemic sclerosis: the emerging role of the antiangiogenic VEGF(165)b splice variant. *Trends Cardiovasc Med* 2011;21:204-10.

39) Distler O, Distler JH, Scheid A, *et al.* Uncontrolled expression of vascular endothelial growth factor and its receptors leads to insufficient skin angiogenesis in patients with systemic sclerosis. *Circ Res* 2004;95:109-16.

40) Rabquer BJ, Koch AE. Angiogenesis and vasculopathy in systemic sclerosis: evolving concepts. *Curr Rheumatol Rep* 2012;14:56-63.

41) Mulligan-Kehoe MJ, Drinane MC, Mollmark J, *et al.* Antiangiogenic plasma activity in patients with systemic sclerosis. *Arthritis Rheum* 2007;56:3448-58.

42) Manetti M, Guiducci S, Romano E, *et al.* Increased plasma levels of the VEGF165b splice variant are associated with the severity of nailfold capillary loss in systemic sclerosis. *Ann Rheum Dis* 2013;72:1425-7.

43) Cébe Suarez S, Pieren M, Cariolato L, *et al.* A VEGF-A splice variant defective for heparin sulfate and neuropilin-1 binding shows attenuated signaling through VEGFR-2. *Cell Mol Life Sci* 2006;63:2067-77.

44) Kawamura H, Li X, Harper SJ, *et al.* Vascular endothelial growth factor (VEGF)-A165b is a weak in vitro agonist for VEGF receptor-2 due to lack of coreceptor binding and deficient regulation of kinase activity. *Cancer Res* 2008;68:4683-92.

45) Ballmer-Hofer K, Andersson AE, Ratcliffe LE, *et al.* Neuropilin-1 promotes VEGFR-2 trafficking through Rab11 vesicles thereby specifying signal output. *Blood* 2011;118:816-26.

46) Chora I, Guiducci S, Manetti M, *et al.* Vascular biomarkers and correlation with peripheral vasculopathy in systemic sclerosis. *Autoimmun Rev* 2015;14:314-22.

14

47) Wu YY, Chen YL, Jao YC, *et al.* miR-320 regulates tumor angiogenesis driven by vascular endothelial cells in oral cancer by silencing neuropilin 1. *Angiogenesis* 2014;17:247-60.

48) Broen JC, Radstake TR, Rossato M. The role of genetics and epigenetics in the pathogenesis of systemic sclerosis. *Nat Rev Rheumatol* 2014;10:671-81.

FIGURE LEGENDS

Figure 1. Serum levels of semaphorin3A (Sema3A) and soluble neuropilin-1 (sNRP1) determined by colorimetric sandwich ELISA. (A) Serum Sema3A levels in healthy controls and patients with systemic sclerosis (SSc). (B) Serum sNRP1 levels in healthy controls and SSc patients. (C) Serum sNRP1 levels in healthy controls and patients with SSc according to nailfold videocapillaroscopy (NVC) pattern (early, active and late). (D) Serum sNRP1 levels in healthy controls and patients with SSc according to the presence/absence of digital ulcers (DU). Data are shown as box plots. Each box represents the 25th to 75th percentiles. Lines inside the boxes represent the median. Lines outside the boxes represent the 10th and the 90th percentiles. Circles indicate outliers, and asterisks indicate the extreme values. Mann-Whitney *U*-test was used for statistical analysis.

Figure 2. Expression of semaphorin3A (Sema3A) in skin biopsies. (A and B) Representative microphotographs of skin sections from (A) healthy controls (n = 11) and (B) systemic sclerosis (SSc) patients (n = 18) immunostained for Sema3A (red) and counterstained with 4′,6-diamidino-2-phenylindole (DAPI; blue) for nuclei. Arrows indicate microvessels. Original magnification: x40. Scale bar = 50 μm. (C) Western blotting of total protein extracts from the skin of healthy subjects (n = 10) and SSc patients (n = 15). A protein band with the expected molecular weight of 90 kDa was detected with the anti-Sema3A antibody. Representative immunoblots are shown. The densitometric analysis of the bands normalised to α-tubulin is reported in the histograms. Data are mean ± SD of optical density in arbitrary units (a.u.).

Figure 3. Expression of neuropilin-1 (NRP1) in skin biopsies. (A, B, D, and E) Representative microphotographs of skin sections from (A and B) healthy controls (n = 11) and (D and E) systemic sclerosis (SSc) patients (n = 18) immunostained for NRP1 (red) and counterstained with 4′,6-diamidino-2-phenylindole (DAPI; blue) for nuclei. Arrows indicate microvessels. (C and F) Representative microphotographs of skin sections from healthy controls (C) and SSc patients (F) double immunostained for NRP1 (red) and the pan-endothelial cell marker CD31 (green) and counterstained with DAPI (blue). Original magnification: x20 (A and D), x40 (B and E), x100 (C and F). Scale bar = 100 μm (A and D), 50 μm (B and E), 10 μm (C and F). (G and H) Western blotting of total protein extracts from the skin of healthy subjects (n = 10) and SSc patients (n = 15). A protein band with the expected molecular weight of 103 kDa was detected with the anti-NRP1 antibody. Representative immunoblots are shown. The densitometric analysis of the bands normalised to α-tubulin is reported in the histograms. Data are mean ± SD of optical density in arbitrary units (a.u.).

Figure 4. (A-D) Expression of neuropilin-1 (NRP1) and Friend leukaemia integration 1 (Fli1) in dermal microvascular endothelial cells (MVECs) and late-outgrowth peripheral blood endothelial progenitor cell (EPC)-derived endothelial cells. (A and C) Western blotting of total protein extracts

15

from healthy MVECs (H-MVECs) at basal condition and treated with recombinant human vascular endothelial growth factor-A165 (VEGF-A165), or 10% serum from SSc patients (n = 5) and healthy subjects (n = 5) for 24 hours, and from basal systemic sclerosis MVECs (SSc-MVECs) assayed with anti-NRP1 (A) and anti-Fli1 (C) antibodies. Representative immunoblots are shown. The densitometric analysis of the bands normalised to α-tubulin is reported in the histograms. Data are mean ± SD of optical density in arbitrary units (a.u.). Student's *t*-test was used for statistical analysis. *p<0.005 *vs.* basal H-MVECs. Results are representative of three independent experiments performed with each one of the 5 H-MVEC and 5 SSc-MVEC lines. (B and D) Western blotting of protein lysates from control (n = 8) and SSc (n = 15) late-outgrowth EPC-derived endothelial cells assayed with anti-NRP1 (B) and anti-Fli1 (D) antibodies. Representative immunoblots are shown. The densitometric analysis of the bands normalised to α-tubulin is reported in the histograms. Data are mean ± SD of optical density in arbitrary units (a.u.). (E) mRNA levels of the Fli1 and NRP1 genes in H-MVECs transfected with Fli1 siRNA or non-silencing scrambled RNA (SCR) were measured by quantitative real-time PCR and normalised to mRNA levels of the 18S ribosomal RNA gene. The relative values compared with SCR are expressed as mean ± SD of three independent experiments. Statistical analysis was carried out with Student's *t*-test. *p<0.01 *vs.* SCR. (F) Chromatin was isolated from H-MVECs and immunoprecipitation was conducted with rabbit anti-Fli1 antibody or rabbit IgG. To exclude exogenous DNA contamination, negative controls were obtained by omitting the cell preparation in some specimens. PCR amplification was carried out using NRP1 promoter-specific primers. One representative of three independent experiments is shown.

Figure 5. *In vitro* angiogenesis. (A) Representative images of capillary morphogenesis on Matrigel after 24 hours. (B) Capillary morphogenesis of healthy and systemic sclerosis (SSc) dermal microvascular endothelial cells (H-MVECs and SSc-MVECs, respectively) quantified as percent field occupancy of capillary projections. Capillary morphogenesis of H-MVECs was evaluated at basal condition and after stimulation with sera from healthy subjects (n = 5) and SSc patients (n = 5), these latter alone or in combination with recombinant human vascular endothelial growth factor-A165 (VEGF-A165) or anti-VEGF-A165b blocking antibodies. Stimulation with VEGF-A165 added to basal medium was used as positive control of angiogenesis. H-MVECs transfected with NRP1 siRNA, at basal condition or challenged with recombinant human VEGF-A165 or VEGF-A165b, or non-silencing scrambled RNA (SCR), were also assayed. Capillary morphogenesis of H-MVECs at basal condition was set to 100%; the other results are normalised to this value. Data are the mean ± SD of three independent experiments performed in triplicate with each one of the 5 H-MVEC and 5 SSc-MVEC lines. Six to 9 photographic fields from 3 plates were scanned for each experimental point. Student's *t*-test was used for statistical analysis. *p<0.01 *vs.* basal H-MVECs; #p<0.05 *vs.* H-MVECs challenged with SSc sera. (C) mRNA levels of the NRP1 gene in H-MVECs transfected with NRP1 siRNA or non-silencing SCR were measured by quantitative real-time PCR and normalised to mRNA levels of the 18S ribosomal RNA gene. The relative values compared with SCR are expressed as mean ± SD of three independent experiments. Statistical analysis was carried out with Student's *t*-test. *p<0.01 *vs.* SCR.

Figure 6. Schematic illustration of the potential mechanisms steering dysregulated angiogenesis in systemic sclerosis (SSc). SSc is characterised by progressive loss of peripheral microvasculature and lack of compensatory angiogenesis. In most angiogenic states, vascular endothelial growth factor-A165 (VEGF-A165) interacts with VEGF receptor-2 (VEGFR-2) *via* the VEGF homology domain (VHD) and with the b1 and b2 domains of neuropilin-1 (NRP1) *via* exons 7 and 8. Co-expression of NRP1 and VEGFR-2 enhances VEGF-A165 binding to VEGFR-2, VEGFR-2 phosphorylation and downstream signalling cascades. In nonangiogenic conditions, such as SSc,

16

both a switch from proangiogenic VEGF-A165 to antiangiogenic VEGF-A165b isoform, which is unable to bind the co-receptor NRP1, and concomitant NRP1 downregulation may result in an insufficient tyrosine phosphorylation/activation of VEGFR-2 and incomplete or transient downstream signalling along with a differential intracellular vesicular trafficking of VEGFR-2 towards the degradative pathway, ultimately leading to an impaired angiogenic response.

17